

Magnetars

Nanda Rea^{a,b} and Davide De Grandis^{a,b}

^aInstitute of Space Sciences (ICE, CSIC), Campus UAB, Carrer de Can Magrans s/n, 08193, Barcelona, Spain

^bInstitut d'Estudis Espacials de Catalunya (IEEC), Esteve Terradas 1, RDIT Building, 08860, Castelldefels, Spain

© 20xx Elsevier Ltd. All rights reserved.

Preprint

Abstract

Magnetars are the most magnetic objects in the Universe, serving as unique laboratories to test physics under extreme magnetic conditions that cannot be replicated on Earth. They were discovered in the late 1970s through their powerful X-ray flares, and were subsequently identified as neutron stars characterized by steady and transient emission across the radio, infrared, optical, X-ray, and gamma-ray bands. In this chapter, we summarize the current state of our experimental and theoretical knowledge on magnetars, as well as briefly discussing their relationship with supernovae, gamma-ray bursts, fast radio bursts, and the transient multi-band sky at large.

Keyword – Compact objects (288); Magnetars (992); Magnetic fields (994); Magnetic stars (995); Neutron stars (1108); Pulsars (1306); Radio pulsars (1353); Soft gamma-ray repeaters (1471); High energy astrophysics (739); Radio transient sources (2008).

Nomenclature

AXP	anomalous X-ray pulsar
(e)MHD	(electron) magneto-hydrodynamics
FRB	fast radio burst
GRB	gamma-ray burst
NS	neutron star
QED	quantum electrodynamics
SGR	soft gamma repeater
XDINS	X-ray dim isolated NS

Key points

- Magnetars are a class of isolated neutron stars characterized by an ultra-strong magnetic field.
- Magnetars were discovered as sources showing flaring X-ray and γ -ray activity (SGRs) and pulsars with anomalously large X-ray luminosity (AXPs).
- Magnetars emit in different energy bands, from radio to γ -rays.
- They exhibit a variety of transient, violent phenomena at high energy.
- They can be used as a laboratory for understanding physics at ultra-high magnetization.
- Recently, magnetars flaring emission or formation have been proposed to power bright extra-Galactic transients.

1 Introduction

The hint for magnetars, a type of neutron star (NS) with extremely powerful magnetic fields dates back to the late 1970s when sudden bursts X/ γ -rays were discovered (Laros et al., 1986), which did not fit the patterns of other celestial sources, i.e. they were repeating, not single events like typical Gamma-Ray Bursts (GRBs). In particular, the 1979 detection of a Giant flare (Mazets et al., 1979, see also section 3) from SGR 0525–66 in the Large Magellanic Cloud was a landmark event to establish the class of sources known as Soft Gamma Repeaters (SGRs), characterized by this very energetic bursting activity.

At that time pulsars were already well known, and their emission mechanism had been linked to the presence of a strongly magnetized, rotating body (Gold, 1968). Indeed, the comparison of pulsar radio timing data to the spin down expected from a rotating magnetic dipole, showed that the bulk of the radio pulsar population was endowed with magnetic fields of $\approx 10^{12}$ G (see figure 1). As large as this value might be for terrestrial standards, these new discoveries following the advent of space-based high-energy instruments, pointed to the existence of even more extreme magnetic sources.

On the other hand, by the 1990s hints of ultra-strong fields were found in a class of persistent X-ray sources with atypically large X-ray luminosity ($\approx 10^{34} - 10^{36}$ erg/s) and whose spin period and spin-down were those of a dipole with $B_d \approx 10^{14}$ G, dubbed Anomalous

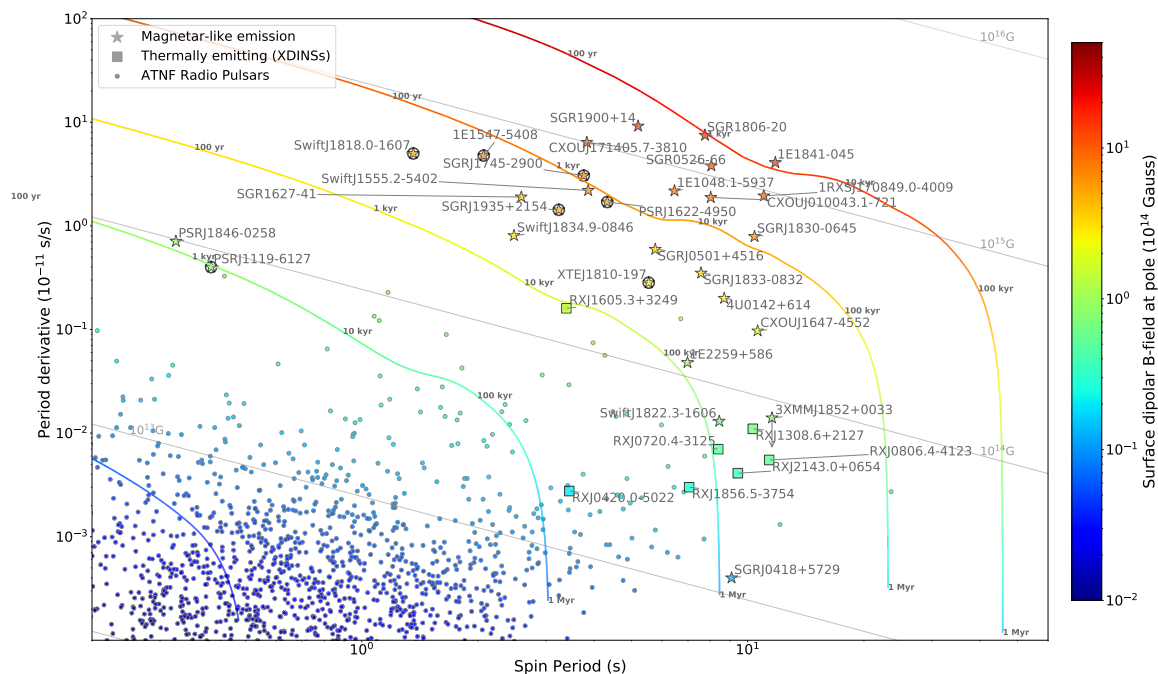


Fig. 1: Period-Period Derivative diagram for different pulsar classes. The color code represent the dipolar magnetic field, and magneto-thermal evolutionary lines are reported for a range of initial magnetic fields. Radio-detected magnetars are marked with a black circle.

X-ray Pulsars (AXPs, Mereghetti and Stella, 1995). These two classes of SGRs and AXPs were unified by Duncan and Thompson (1992); Thompson and Duncan (1993) under the *magnetar* paradigm. Later on, the measure of the X-ray quiescent state of SGRs with distinctive spin periods (Kouveliotou et al., 1998, 1999), and the detection of bursting activity from some known AXPs (Gavriil et al., 2002), further rendered the distinction obsolete, well establishing magnetars as a proper class of pulsars.

Thus, we can define a magnetar as a pulsar whose emission, both during transient, violent episodes and its persistent state, is powered by a strong magnetic field. Their spin periods range between ≈ 0.3 -12 s with relatively large period derivatives ($\dot{P} \sim 10^{-13} - 10^{-9}$ s s $^{-1}$; see figure 1). This is often reflected in a high value of their magnetic fields as obtained from timing measurements, $B_d \gtrsim 10^{14}$ G. This field is often larger than the *critical quantum field*, i.e. the one at which the cyclotron energy $\hbar\omega_B = \hbar eB/m_e c$ of an electron is equal to its rest mass energy $m_e c^2$, $B_Q = m_e^2 c^3 / e \hbar \approx 4.414 \times 10^{13}$ G. These large fields are making magnetars ideal laboratories for the study of quantum electro-dynamics and plasma physics under strong field regimes. Nevertheless, while the spin-down field is generally a good proxy for the actual field strength, and indeed most sources have $B_d \gtrsim B_Q$, see figure 1, it must be born in mind that B_d is an estimate of the dipolar part of the poloidal field component, and most of the magnetic energy may well be stored in higher multipoles and/or the toroidal component. An outstanding illustration of this fact comes from the discovery of the low field magnetars, which despite having a spin-down field more akin to normal pulsars, they underwent magnetar-like bursting episodes (Rea et al., 2010, 2012a, see also section 3).

At the time of writing, 29 sources have been unequivocally identified as magnetars, all in our Galaxy or in the Magellanic Clouds (see figure 2). Extensive reviews about magnetars, both from observations and theoretical perspectives, can be found in Turolla et al. (2015a); Kaspi and Beloborodov (2017); Mereghetti et al. (2018); Esposito et al. (2021).

2 Magnetars' steady emission

2.1 X-rays and γ -rays

Magnetars' persistent X-ray emission is where most of their energy is released. In the 0.5–100 keV energy range, magnetar spectra are consistently well described by one or two thermal blackbody components, often accompanied by one or two power-law components (see also figure 3). Most magnetar spectra do not reach energies above 10 keV, with some exceptions that can instead be visible up to hundreds of keV. The X-ray luminosity of magnetars in quiescence ranges between 10^{31-35} erg s $^{-1}$ and it is believed to originate from thermal processes. The blackbody spectral models have a temperatures in the $kT \approx 0.15$ –1 keV. These temperatures are significantly higher than that of typical

Table 1: Timing properties and timing-inferred parameters, and physical properties of the current sample of known magnetars.

Source	P (s)	\dot{P} (10^{-11} s s $^{-1}$)	$B_{p,dip}^a$ (10^{14} G)	\dot{E}_{rot}^b (erg s $^{-1}$)	τ_c^c (kyr)	D (kpc)	Association	Bands ^d	Reference
SGR 0526–66 [†]	8.05	3.8	11.0	2.9×10^{33}	3.4	49.7	SNR N49 (LMC)	X	Olausen and Kaspi (2014)
SGR 1900+14 [†]	5.20	9.2	14.0	2.6×10^{34}	0.9	12.5	cluster	γ X O	Olausen and Kaspi (2014)
SGR 1806–20 [†]	7.55	76.95	49	7.0×10^{34}	0.2	8.7	cluster W31	γ X O	Younes et al. (2015)
1E 2259+586	6.98	0.048	1.2	1.3×10^{32}	230	3.2	SNR CTB109	γ X O I	Dib and Kaspi (2014)
1E 1048.1–5937	6.46	2.18	7.6	3.2×10^{33}	4.7	9		γ X O	Dib and Kaspi (2014)
4U 0142+614	8.69	0.20	2.7	1.3×10^{32}	69	3.6		γ X O I	Olausen and Kaspi (2014)
1E 1841–045	11.79	4.09	13.8	9.9×10^{33}	4.6	8.5	SNR Kes73	γ X O	Olausen and Kaspi (2014)
1RXSJ170849.0–4009	11.01	1.95	9.3	5.8×10^{32}	9.1	3.8		γ X O	Olausen and Kaspi (2014)
SGR 1627–41 ^e	2.59	1.9	4.5	4.3×10^{34}	2	11	SNR G337.0-0.1	X I	Esposito et al. (2009)
XTE J1810–197	5.54	0.283	2.6	6.7×10^{32}	31	3.5		X O I R	Camilo et al. (2016)
CXOU J010043.1–721	8.02	1.88	7.9	1.4×10^{33}	6.8	62.4	SMC	X O	Olausen and Kaspi (2014)
CXOU J164710.2–455216	10.61	0.097	2.1	3.2×10^{31}	173	4	cluster Wd1	X	Rodríguez Castillo et al. (2014)
PSR J1846–0258	0.33	0.71	0.98	8.1×10^{36}	0.7	6.0		γ X	Viganò et al. (2013))
1E 1547–5408	2.07	4.77	6.4	2.1×10^{35}	0.7	4.5	SNR G327.24-0.13	γ X O R	Dib et al. (2012)
SGR 0501+4516	5.76	0.594	3.7	1.2×10^{33}	15	1.5	SNR G160.9+2.6	γ X O	Camero et al. (2014)
SGR 0418+5729	9.08	0.0004	0.1	2.1×10^{29}	~ 36000	2		X	Rea et al. (2013)
SGR 1833–0832	7.57	0.35	3.3	3.2×10^{32}	34	10 ^f		X	Esposito et al. (2011)
PSR J1622–4950	4.33	1.7	2.7	8.3×10^{33}	4.0	9	SNR G333.9+0.0	X R	Levin et al. (2010)
CXOU J171405.7–3810	3.83	6.40	10.0	4.5×10^{34}	0.95	13.2	SNR CTB37B	X	Olausen and Kaspi (2014)
Swift J1834.9–0846	2.48	0.806	2.9	2.1×10^{34}	5	4.2		X	Esposito et al. (2013)
Swift J1822.3–1606	8.44	0.013	0.7	8.4×10^{30}	1030	1.6		X	Rodríguez Castillo et al. (2016)
SGR 1745–2900	3.76	3.06	6.9	2.2×10^{34}	1.9	8.3	Galactic centre	γ X R	Coti Zelati et al. (2017)
3XMM J185246.6+003317	11.56	< 0.014	< 0.41	$< 3.6 \times 10^{30}$	> 1300	7.1		X	Rea et al. (2014)
SGR 1935+2154	3.24	1.43	4.4	1.6×10^{34}	3.6	9		γ X R	Israel et al. (2016)
PSR J1119–6127	0.41	0.4	0.82	2.5×10^{36}	1.6	8.4	SNR G292.2–0.5	X R	Viganò et al. (2013)
1E 161348–5055	24030	<70	<2600	$< 2 \times 10^{24}$	> 540	3.3	SNR RCW 103	X	Rea et al. (2016)
SGR J1830–0645	10.42	0.7	5.5	2.4×10^{32}	24	10 ^f		X	Coti Zelati et al. (2021)
Swift J1818.0–1607	1.36	9	3.5	1.4×10^{36}	0.24	4.8		γ X R	Esposito et al. (2020)
Swift 1555.2–5402	3.86	3.05	3.47	2.09×10^{34}	2.01	10 ^f		X	Enoto et al. (2021)

[†] Underwent a giant flare (see section 3).

^a Assuming a force-free magnetosphere and an aligned rotator, a star radius $R = 10$ km and moment of inertia $I = 10^{45}$ g cm 2 , the dipolar component of the surface magnetic field at the polar caps is given by $B_{p,dip} \sim 2 \cdot (3c^3 I P \dot{P} / 8\pi^2 R^6)^{1/2} \sim 6.4 \times 10^{19} (P \dot{P})^{1/2}$ G. Relativistic magnetohydrodynamic simulations of pulsar magnetospheres have shown that the estimate offered by this formula is correct within a factor of $\sim 2 - 3$ (Spitkovsky 2006).

^b With the same assumptions, the rotational energy loss is given by $\dot{E}_{rot} = 4\pi^2 I \dot{P} P^{-3} \sim 3.9 \times 10^{46} \dot{P} P^{-3}$ erg s $^{-1}$.

^c With the same assumptions and assuming that the spin period at birth was much smaller than the current value, the characteristic age is given by $\tau_c = P/2\dot{P}$.

^d γ =soft gamma/hard X, X=X-rays, O=optical, I=infrared, R=radio.

^e The spin period and its derivative were detected only following the 2008 re-activation of the source. We assume the same spin period derivative also for the 1998 outburst, and consider the same values for $B_{p,dip}$, \dot{E}_{rot} and τ_c in our searches for correlations.

^f The value for the distance is assumed.

rotation-powered pulsars being powered by the secular decay of their high magnetic fields in the crust (see section 5 and figure 6). For the same reason, X-rays magnetars are usually more luminous than rotation-powered pulsars of similar characteristic age, since their surfaces get continuously heated by the decay of the magnetic field (e.g. Aguilera et al., 2008; Viganò et al., 2013; Gourgouliatos et al., 2016; De Grandis et al., 2020; Igoshev et al., 2020; Dehman et al., 2023). Interestingly, the blackbody fitted to the magnetars' X-ray spectra often indicate a thermal emission region much smaller than the stellar surface. This suggests that using a single-temperature blackbody model might be an oversimplification. Strong magnetic fields in the star's crust could lead to substantial temperature anisotropies (e.g. Gourgouliatos et al., 2016; Igoshev et al., 2020). These small, highly heated areas could result from particle bombardment by magnetospheric currents, driven by large-scale twists in the external magnetic field or local internal twist kept stable by the internal field helicity.

Regardless of the origin, the thermal emission is likely affected by the presence of a magnetized atmosphere and by magnetospheric processes, such as resonant cyclotron scattering by charged particles. Since the particles are distributed across vast regions of the magnetosphere, which have varying magnetic field strengths, this scattering process generates a broad spectral hardening, rather than narrow lines or distinct harmonics. The two power-laws components present in some objects have photon index within the ranges of $\Gamma_{soft} \sim 2-4$ (in the 0.5–10 keV soft X-ray energy range) and $\Gamma_{hard} \sim 0.5-2$ (in the 10–200 keV hard X-ray energy range). Whereas the soft X-ray non-thermal component was discovered alongside the first magnetar X-ray counterparts, the hard X-ray components have been observed only several decades thereafter, thanks to the advent of sensitive instrument in the 2000's, namely *INTEGRAL*, *Suzaku*, and *NuSTAR* (Kuiper et al., 2004, 2006; Götz et al., 2006, 2007; den Hartog et al., 2008b,a; An et al., 2014; Enoto et al., 2017). At even higher energies, upper limits derived at MeV, GeV and even TeV energies observations with *CGRO*, *Fermi*, and *HESS* suggest that these hard power-law compo-

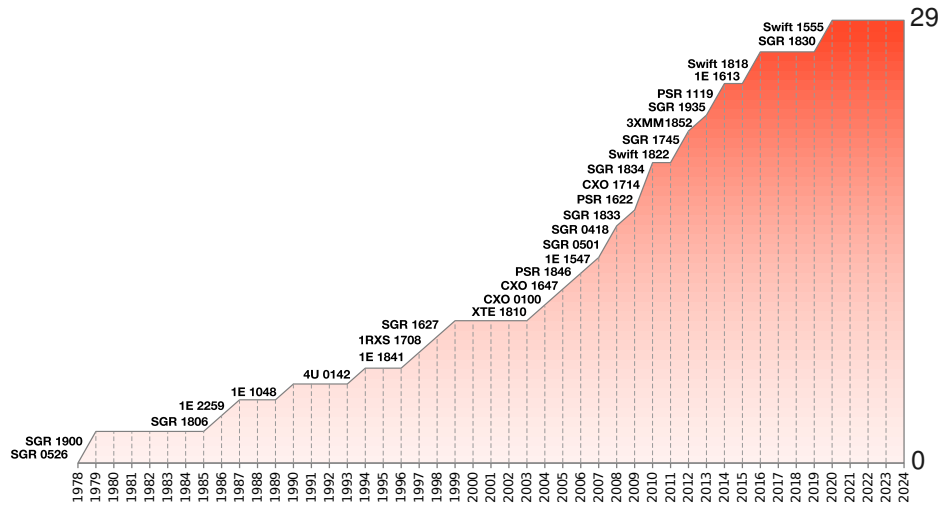


Fig. 2: Magnetars discoveries as a function of time. See table 1 for the complete names, which are given here in shortened form.

nents do not persist beyond ~ 500 keV (e.g. den Hartog et al., 2008b; Li et al., 2017; Aleksić et al., 2013). They can vary with the pulse phase, and in time when the source is undergoing an outburst, but their luminosity is generally comparable to or even greater than that found below 10 keV. The exact origin of magnetar non-thermal soft and hard X-ray emission, modeled by the two power-laws, is still debated. However, it is generally thought that they are produced by up-scattering photons off non-relativistic (for the Γ_{soft}) and ultra-relativistic electrons (for the Γ_{hard}) (Baring and Harding, 2007; Fernández and Thompson, 2007; Wadiasingh et al., 2018) potentially linked to relativistic outflows occurring in the NS magnetosphere (Beloborodov, 2013). Note that all these spectral components are necessarily modulated by a substantial interstellar photoelectric absorption in the line of sight, given that all Galactic magnetars lie within the Galactic plane.

The X-ray emission of magnetars is modulated by their spin, showing single, double or even triple peak pulse profiles, depending on the distribution of the X-ray emission region. Moreover, variations in pulse profiles and energy-dependent shifts in the pulse peaks are observed across different phases (den Hartog et al., 2008a; Götz et al., 2007). Magnetars' analysis of the evolution of the spin period in time have revealed large timing noise and the presence of glitches in many cases (Dib et al., 2008). The strong and unstable twisted magnetosphere of these objects leave a chaotic imprint in their timing stability.

2.1.1 X-ray polarization

The launch of the *IXPE* satellite in 2021 allowed for the first time to perform a long program of polarization measurements in the X-ray band. As polarization is associated to strong magnetism, magnetars were a natural target for this instrument, even though the large number of photons required to resolve spectral and polarization features made so that only the brightest ones could be observed (see the review in Taverna and Turolla, 2024).

Magnetars were indeed to be strongly polarized, with integrated polarization degrees of $10\% \lesssim PD \lesssim 35\%$, reaching up to $\approx 80\%$ in confined energy bands (as in the case of 1RXS J170849.0-400910, the most strongly polarized source observed by *IXPE* to date). Moreover, in the case of the brightest magnetar, 4U 0142+61, the polarization angle has been observed to strongly depend on energy, with a 90° swing between low and high energy as shown in Fig. 3; this points towards the fact that different regions on the surface of the magnetar have with rather different optical properties (see section 4.1).

2.2 Optical and IR

Roughly a third of all known magnetars have detected counterparts in the optical or infrared bands (see table 1), though identifying these is challenging due to their intrinsic faintness ($K \sim 21$ mag, and $V \sim 24$ mag) and the Galactic reddening in the disk, where all magnetars lie. During long-term outbursts, the infrared and optical variability of magnetars does not consistently correlate with their X-ray flux, possibly due to limited multi-wavelength observation campaigns, resulting in reports of both correlated and erratic variation patterns (Hulleman et al., 2004; Rea et al., 2004; Tam et al., 2004). Some associations are firmly established through spin modulation in the optical band, seen in sources like 4U 0142+61, 1E 1048.1-5937, and SGR J0501+4516 (Kern and Martin, 2002; Dhillon et al., 2011), with additional long-term variability strengthening these associations in other cases. For 4U 0142+61, a significant dataset recorded with the James Webb telescope, Hubble and the major terrestrial telescopes in the infrared and optical bands, suggests a peculiar spectral decomposition. Some years ago, it was proposed the presence of a multi-temperature disk potentially formed from supernova fallback material and passively heated by the magnetar's X-rays, aligning with observed X-ray and infrared emission correlations (Hare et al., 2024). However, magnetospheric origin theories also exist, with models suggesting that the curvature radiation in a pair-dominated inner magnetosphere could produce the observed infrared/optical luminosity and explain optical pulsations (see figure 4). Recent James Webb observations supports this latter scenario Hare

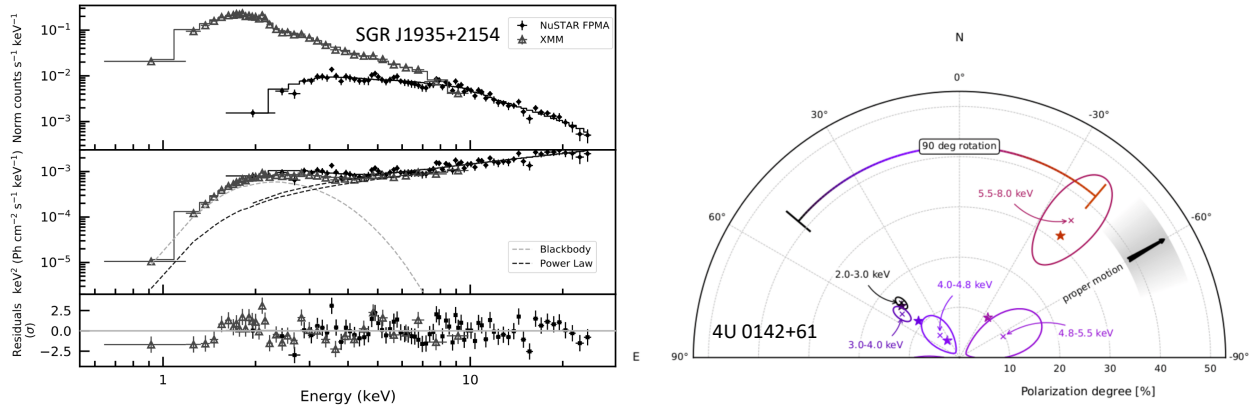


Fig. 3: Soft and hard X-ray spectrum of SGR 1935+2154 (Borghese et al., 2022); X-ray polarimetry detected by *IXPE* for 4U 0142+61 Taverna et al. (2022).

et al. (2024). The optical and infrared pulsations appear nearly aligned with X-ray profiles, exhibiting broad modulation and substantial pulsed fractions.

2.3 Radio

A subset of magnetars also emits in the radio band. Radio emission from magnetars has been discovered in 2006 (Camilo et al., 2006) following the discovery of the first X-ray outburst from these objects (Ibrahim et al., 2004a, and section 3). Radio-emitting magnetars show intermittent or episodic bursts, always coinciding with X-ray outbursts.

The mechanisms behind magnetar radio emission is still unknown, but the relatively high rotational power of radio magnetars compared to their peers might suggest a similar rotation-powered origin as for traditional pulsars (Rea et al., 2012b, see also figure 6). However, while typical radio pulsars exhibit stable pulse profiles, steep inverted spectra and stable fluxes, the emission profiles of radio magnetars are variable and complex, characterized by highly dynamic and powerful bursty peaks. Unlike the predictable radio signals from pulsars, magnetar radio pulses can show extreme variability in brightness, spectral properties, and polarization. For example, XTE J1810–197 displays unusual spectral behavior (see figure 4), such as rapid shifts in pulse profiles and strong polarization, suggesting that its radio emissions may originate from processes specific to the magnetar’s intense magnetic field.

Moreover, radio-emitting magnetars have been observed with very high brightness temperatures, comparable to those of fast radio bursts (FRBs), leading to speculations that magnetars might also be sources of some FRB events. Most notably, the Galactic magnetar SGR J1935+2154 exhibited a burst with FRB-like properties in 2020, providing a compelling link between magnetar activity and FRBs (Mereghetti et al., 2020). The polarization and temporal structures of these emissions are actively studied, as they offer insights into the geometry and magnetospheric processes of magnetars, which differ markedly from those seen in standard pulsars.

Another trait sometimes found in magnetars with radio emissions is the transition between radio-loud and radio-quiet states, often triggered by energetic events or outbursts (see section 3) in higher-energy bands. This transition suggests a close coupling between the magnetar’s magnetic field dynamics and its radio emission capability, once more hinting at unique emission mechanisms directly tied to its powerful magnetic field and the surrounding plasma environment (Archibald et al., 2017).

3 Magnetar’s flaring and outbursts

The flaring activity of magnetars is a distinctive property of these highly magnetic NS, setting them apart from other types due to their unpredictable explosive behavior. Short flaring episodes are often associated with a general increase of the luminosity of these objects, lasting months to years, usually called outbursts. From an observational perspective, magnetars transient activity can fall into three main (strongly related) categories (see also figure 5):

- **X-ray/ γ -ray Short Bursts.** These are the most frequent and least energetic flares. Short bursts are brief (lasting about 0.1–0.2 seconds), have thermal spectra, and peak at luminosities of $10^{38} - 10^{40}$ erg/s, much higher than the Eddington limit for typical NS. Short bursts are irregular in timing, occurring singly or in clusters (Kaspi et al., 2003; Woods et al., 2005).
- **Intermediate Flares.** These events have durations between short bursts and giant flares, ranging from around 1–60 seconds, with luminosities reaching $10^{41} - 10^{42}$ erg/s. Some intermediate flares last longer than the magnetar’s spin period, showing clear pulsation at the NS’s spin frequency. Such events are seen in SGRs but have not yet been confirmed in AXPs.
- **Giant Flares.** Giant flares are among the most energetic known flaring events in our Galaxy, reaching $10^{43} - 10^{45}$ erg/s and rivaling only supernova explosions. Only three have been recorded: in 1979 from SGR J0526–66, in 1998 from SGR 1900+14, and in 2004 from

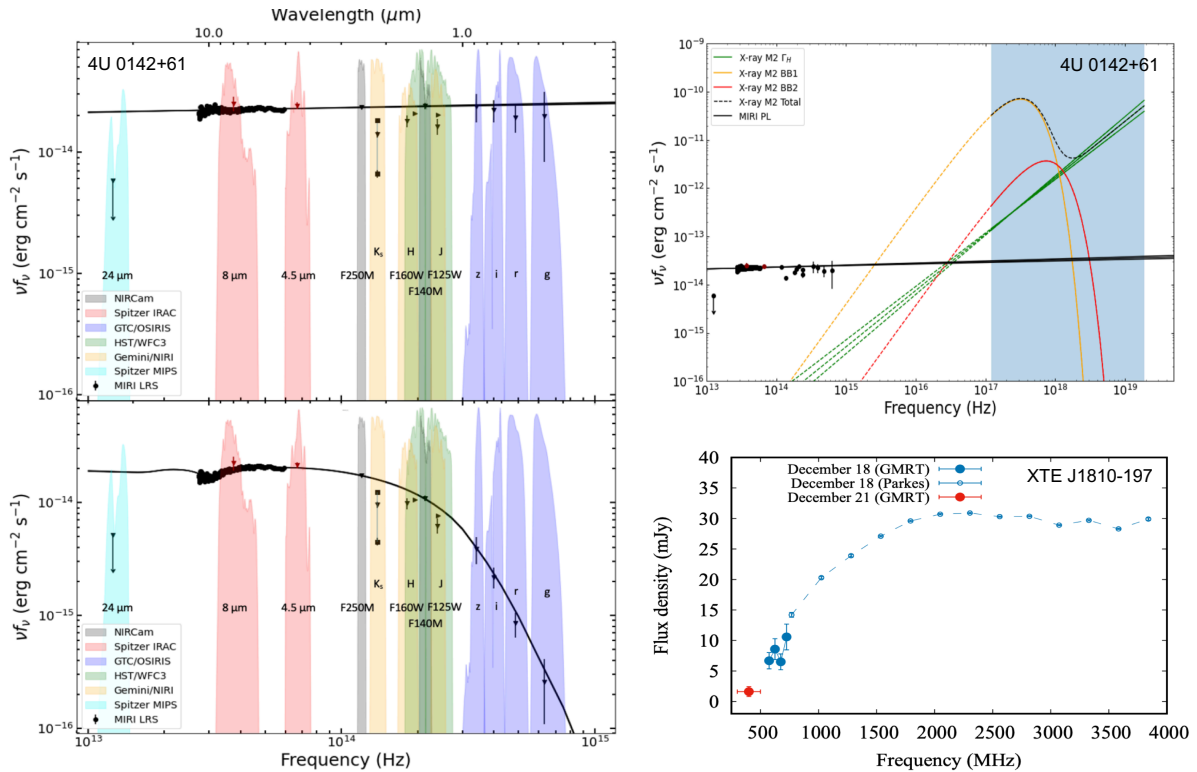


Fig. 4: Multi-band spectrum of 4U 0142+61 as observed by the James Webb telescope (Hare et al., 2024). Bottom-right panel show the radio spectrum of XTE J1810-197 (Maan et al., 2022).

SGR J1806–20. Each of these flares featured a short, intense peak lasting under a second, followed by a long, pulsating tail (spanning hundreds of seconds) that aligns with the NS’s spin period (Turolla et al., 2015b, and reference therein). Moreover, some high energy events in spatial coincidence with a known nearby galaxy have been identified as magnetar giant flares; in particular, recently a giant-flare-like event has been observed in the M82 galaxy, and for the first time a prompt multi-wavelength campaign was able to exclude a GRB origin for it (Mereghetti et al., 2024).

• **Outbursts.** Transient events are a defining feature of magnetars, acting as key indicators of their presence and contributing significantly to new discoveries in this category of NS. Since the identification of the first transient magnetar event in July 2003 (Ibrahim et al., 2004b), the count of magnetars has grown by a third within six years, largely due to these episodic outbursts (figure 2 and Rea and Esposito, 2011; Coti Zelati et al., 2018a). To date, about 20 magnetar outbursts have been observed, displaying a varied phenomenology, each giving valuable insights into their unique nature.

During an outburst, magnetars can exhibit enhanced emissions across multiple bands, from radio to hard X-rays, with soft X-ray fluxes typically increasing by factors of 10 to 1000 relative to their quiescent levels. This flux increase is often accompanied by spectral evolution, where the X-ray spectrum tends to soften as the outburst decays. Decay timescales for these events vary widely among sources, lasting anywhere from a few weeks to several years. The decay profile can follow different patterns, some resembling an exponential decay, others a power-law, and some requiring more complex models with multiple components to describe the flux decrease over time (see figure 8). Recent multi-band observations have advanced our understanding of these outbursts, showing that the emission properties evolve across the spectrum during outburst phases. Furthermore, some outbursts exhibit enhanced radio and optical activity in addition to X-rays, providing clues about the magnetospheric processes and extreme magnetic fields that drive these events (Ibrahim et al., 2004b; Rea et al., 2013; Younes et al., 2017; Coti Zelati et al., 2018b; Borghese et al., 2021; Younes et al., 2021; Ibrahim et al., 2024).

4 Modeling Magnetars

4.1 Modeling spectra

As mentioned in section 2, the spectrum of a magnetar is the result of thermal photons emitted from the hot surface that then interact with a complex magnetosphere. The energy scale of the emission is thus determined by the temperature of the star, whose evolution is described in section 5; in the following, the processes behind the shape of the spectrum will be reviewed.

The thermal component arising from the cooling of the NS surface is often modeled in terms a single BB component for simplicity.

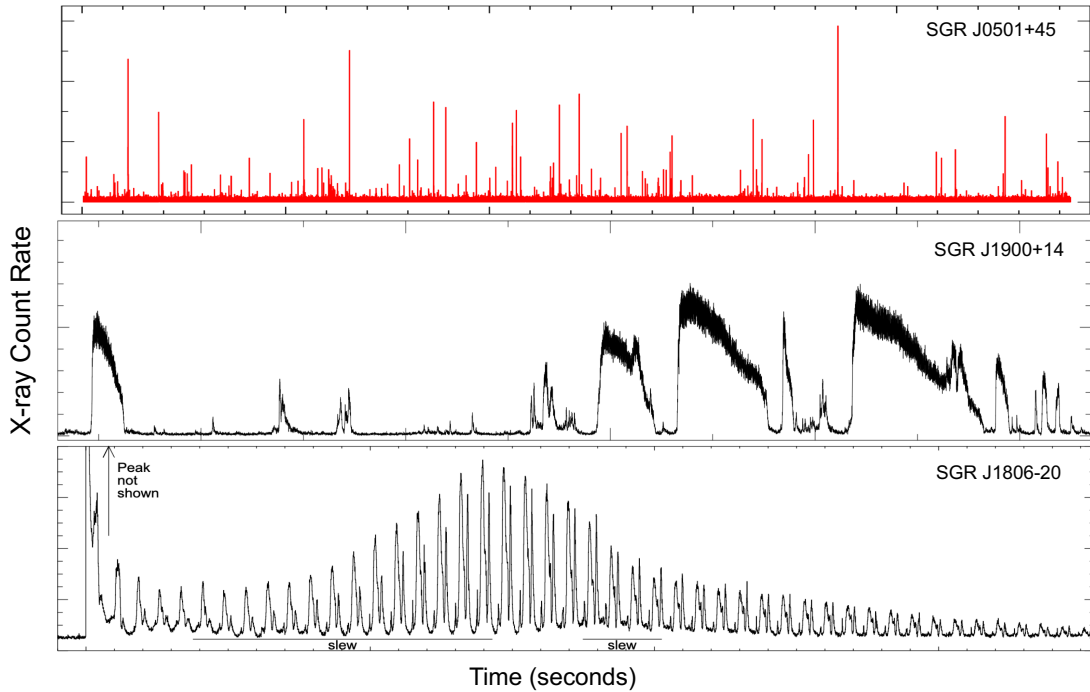


Fig. 5: X-ray flaring activity of magnetars (from top to bottom): short X-ray flares (Rea et al., 2009), intermediate flares (Israel et al., 2008) and a giant flare (Palmer et al., 2005).

However, the outermost layers of the surface can have non-trivial optical properties, shaping the spectrum beyond this simple model. In particular, the surface of a magnetar can be covered by a thin gaseous atmosphere, which broadens the spectrum, or lay bare. The latter case is the result of the condensation of the surface induced by the magnetic field (Ruderman, 1974): as the Lorentz force on electrons becomes comparable of exceeding the electrostatic attraction exerted by the nucleus, atomic orbitals get deformed to an oblong shape, acquiring a different set of quantum numbers with respect to the non-magnetized case; these cylinder-like orbitals can also form covalent bonds between each other, resulting in long chains of atoms bond along field lines (*polymerization*) that then interact to form a solid. The complexity of treating theoretically the properties of this transition, which occurs in a regime entirely inaccessible to ground-based experiments, has produced a range of diverse estimates (e.g. Flowers et al., 1977; Jones, 1986; Neuhauser et al., 1987; Fushiki et al., 1992; Medin and Lai, 2006); because of this, the density of the condensed phase of a species with atomic and mass numbers Z and A is expressed within the literature as (Potekhin and Chabrier, 2013)

$$\rho_s = 561 \xi AZ^{-0.6} \left(\frac{B}{10^{12} \text{ G}} \right)^{1.2} \text{ g cm}^{-3}, \quad (1)$$

where $\xi \approx 1$ is an uncertainty parameter reflecting different estimates. Even more uncertain is the critical temperature of this transition; as an example, Potekhin and Chabrier (2013) describe the results by Medin and Lai (2006) as $T_c = 5 \times 10^4 Z^{1/4} (B/10^{12} \text{ G})^{3/4} \text{ K}$. At any rate, the emission from a condensed surface is quite different from an atmosphere; from a spectral point of view, it is much more similar to a pure BB (e.g. Turolla et al., 2004). Moreover, the two situation differ in their polarization properties, as an atmosphere is expected to strongly polarize radiation ($\text{PD} \gtrsim 70\%$) mainly in the X-mode (i.e., perpendicularly to the field direction), whereas a condensed surface can only reach $\text{PD} \lesssim 30\%$ in a direction that varies with the energy and the field orientation (Taverna and Turolla, 2024, and references therein, see also section 2.1.1).

Within a strongly magnetized plasma, the electron scattering cross section acquires an additional *resonant cyclotron scattering* (RCS) contribution proportional to (e.g. Canuto et al., 1971)

$$\sigma_T \frac{\omega^2}{(\omega - \omega_B)^2 + \Gamma^2/4} \quad (2)$$

where σ_T is the Thomson cross-section, α is the angle between the electron momentum and the magnetic field and $\Gamma = 4e^2\omega_B^2/3m_e c^3$ is the natural line width (i.e., the inverse of the characteristic time of the transition between adjacent Landau levels); in astrophysical conditions, this width is generally smaller than the Doppler width $\Delta\omega = \beta_{\parallel}\omega_B$, where $\beta_T = (k_B T_{\parallel}/m_e c^2)^{1/2}$ with the temperature T_{\parallel} being computed over the distribution of momenta parallel to the field (Zheleznyakov, 1996). This produces an absorption line in the spectrum, which has indeed been detected in some sources (e.g. the proton line in the spectrum of the low-B magnetar SGR 0418+5729 Tiengo et al., 2013); however, in the most typical magnetar cases the field structure is so complex that rather than a finite set of well-defined lines the combined results is a power law continuum, superimposed to the initial thermal distribution.

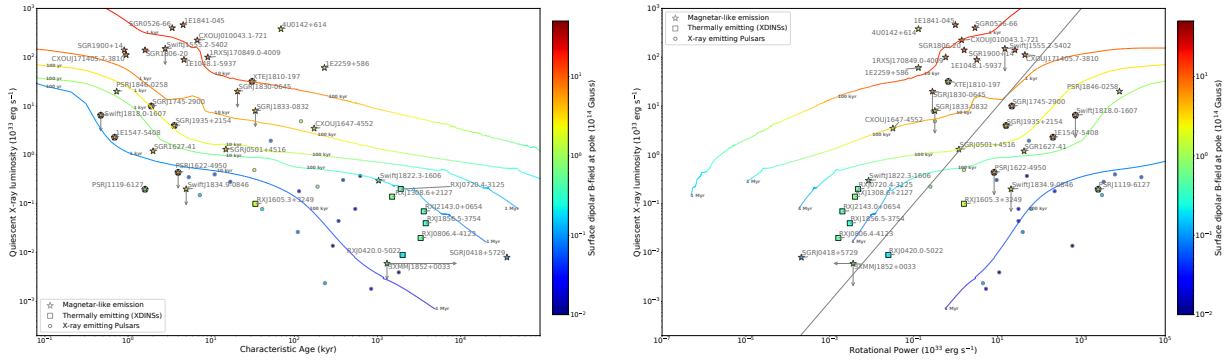


Fig. 6: Thermal X-rays luminosity as a function of the characteristic age $\tau = P/2\dot{P}$ (left) and rotational power $\dot{E} \propto \dot{P}/P^3$ (right). The theoretical models are the same as Figure 1.

The first attempt to characterize soft-X magnetar spectra in these terms was performed by the 1D model (Lyutikov and Gavriil, 2006; Rea et al., 2008), which despite a number of simplifying assumptions has the advantage of producing a manageable analytical model. In particular, they consider only the Thomson cross section to describe the scattering, which is only adequate in the non relativistic regime, low field regime. When considering the harder part of the spectrum $\gtrsim 10$ keV, the cross section must take into account relativistic and quantum electrodynamics effects, as well as those of the ultra strong field when B is comparable or above B_Q and electron can inhabit different Landau levels. A similar physical mechanism is invoked to account for the power law emerging in the harder X-rays, above ~ 10 keV. Namely, photons populate this energy range when undergo *resonant inverse Compton scattering* (RICS), in which the interaction of thermal photons with highly energetic electrons in the magnetosphere upscatters them (e.g. Nobili et al., 2008; Zane et al., 2009; Baring et al., 2021, and references therein).

4.2 The evolution of the magnetic field

The enormous strength of the magnetic field in magnetars very effectively slows down their rotation via the emission of braking radiation, which is reflected by them lying at the top-right corner of the $P\dot{P}$ diagram. Still, their periods are observed not to exceed ~ 10 seconds. This fact can be accounted for by considering the decay of the magnetic field over the life of the magnetar; the observed values are then recovered when accounting for a highly resistive layer, likely composed of nuclear pasta in the inner crust (Pons et al., 2013).

Under the conditions found in a NS, matter is in general a very good electrical conductor (see Potekhin et al., 2015, for a review of NS microphysical properties) but its conductivity is nonetheless finite, hence dissipation is taking place. A crucial aspect of this problem is that the conductivity depends on the temperature and dissipation in turn produces heat, making the magnetic and thermal evolution two strongly coupled problems (e.g. Wiebicke and Geppert, 1996; Gourgouliatos et al., 2016; Pons and Viganò, 2019; De Grandis et al., 2020; Igoshev et al., 2020; Dehman et al., 2023; Ascenzi et al., 2024, and references therein).

For what concerns the magnetic field structure, a magnetar can be divided in two main region, the solid crust and the core. The latter is likely in some kind of superfluid/superconducting state, as indicated by the proneness of magnetars to (anti)glitch (e.g. Antonopoulou et al., 2022, and references therein), in which the field gets constrained in flux tubes that have a poorly understood dynamic. More work has been done in the crust, where the bulk of the magnetization is believed to reside; there, the problem can be treated in the eMHD regime, in which the induction equation (neglecting for simplicity GR corrections) reads

$$\frac{\partial \mathbf{B}}{\partial t} = -\nabla \times \left[\frac{c^2}{4\pi\sigma} \nabla \times \mathbf{B} + \frac{c}{4\pi n_e} (\nabla \times \mathbf{B}) \times \mathbf{B} \right]; \quad (3)$$

the first term on the RHS describes ohmic dissipation, whereas the second is known as the Hall effect. The latter is non-dissipative, but acts by transferring energy between poloidal and toroidal field components and between different multipoles, most notably in the case of NSs towards the smaller scales in the so-called *Hall cascade*, Goldreich and Reisenegger, 1992; this can in turn affect dissipation, which is more efficient for the higher multipoles. Moreover, the Hall term is prone to produce MHD instabilities (Wood et al., 2014), which can dramatically enhance the production of small scale structures (Gourgouliatos et al., 2016; De Grandis et al., 2020). By computing the scale values in to the two terms in Eq. 3, one can define the timescales for the two processes as

$$\begin{aligned} \tau_H &= \frac{4\pi n_e c L^2}{cB} \approx 6.6 \times 10^4 \left(\frac{n}{10^{34} \text{ cm}^{-3}} \right) \left(\frac{B}{10^{13} \text{ G}} \right)^{-1} \left(\frac{L}{1 \text{ km}} \right)^2 \text{ yr} \\ \tau_O &= \frac{4\pi\sigma}{c^2} L^2 \approx 4.4 \times 10^6 \left(\frac{\sigma}{10^{24} \text{ s}^{-1}} \right) \left(\frac{L}{1 \text{ km}} \right)^2 \text{ yr} \end{aligned} \quad (4)$$

where the numerical values were computed assuming typical values for the crust of a magnetar. The two mechanisms are hence operating over quite different timescales; moreover, the field dissipation time does not explicitly depend from the field itself. In figure 1, we show

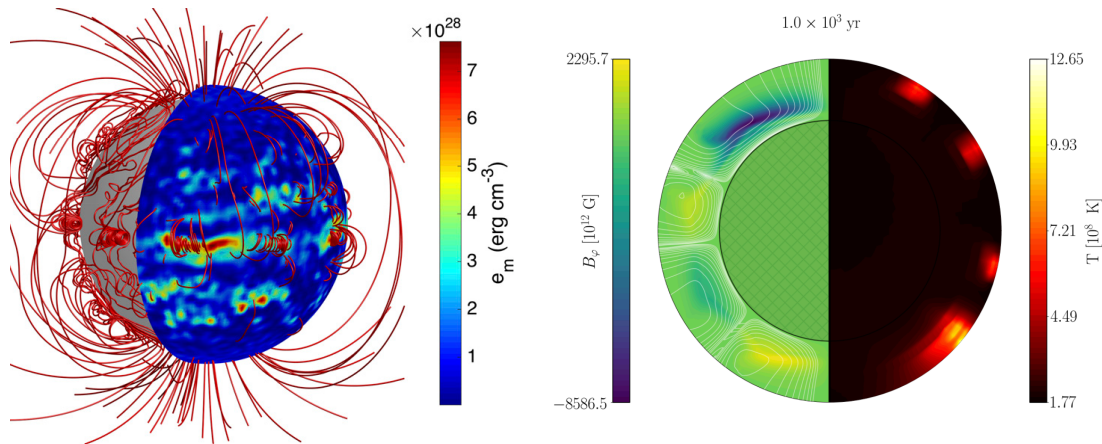


Fig. 7: (Left) Magnetic field lines and surface energy after 15 kyr of the 3D Hall evolution of a field having initially a very small degree of asymmetry (10^{-4} of the total energy in the asymmetric part); from Gourgouliatos et al. (2016). (Right) Example of magnetothermal simulation of a young NS in axial symmetry (the crust is enlarged by a factor 8 for visualization). The coupled evolution leads to the formation of small scale thermal and magnetic features; from Dehman et al. (2020).

a set of NS evolutionary tracks on the $P\dot{P}$ diagram; in the early phases, they almost follow a line of constant characteristic field, but then progressively diverge, and after ~ 100 kyr the field decay is so substantial that there is almost no increase in period. This is indeed reflected by observations, as no magnetars with a period larger than ~ 20 s are observed.

A major problem in setting up simulations of magnetic field evolution is represented by the choice of the initial conditions. In fact, it is not clear at present what physical mechanism is responsible for the creation of a magnetar-strength field, and hence what kind of topology is to be expected in a newborn magnetar. In fact, the conservation of the magnetic flux during the core-collapse of the progenitor (*fossil field scenario*, e.g. Ferrario and Wickramasinghe, 2006) might be able to sizably amplify the magnetic field, but the available data on stellar field do not seem to be able to account for the strong fields found throughout the magnetar population (Makarenko et al., 2021). Another possibility is that the fossil field act as the seed for some kind of dynamo in the proto-NS phase, when the star is spinning extremely fast; still, no consensus on the exact mechanism has been reached, the main candidates being the convective dynamo (as in the original work by Thompson and Duncan, 1993, see also Bonanno et al., 2003; Masada et al., 2022; White et al., 2022), the magnetorotational instability (MRI) driven dynamo (e.g. Obergaulinger et al., 2009; Reboul-Salze et al., 2021, 2022) and the Tayler-Spruit dynamo in a PNS spun by fallback material (Barrère et al., 2022, 2024). More recently, Dehman and Brandenburg (2024) showed that under certain conditions the field evolution described by Eq. 3 may on its own induce an inverse cascade boosting the dipolar field. At any rate, it appears clear that the formation and evolution of ultra-strong fields involves complex topologies, producing structures spanning several scales, as illustrated in figure 7 (left panel, from Gourgouliatos et al., 2016, see also De Grandis et al., 2022; Dehman et al., 2023).

Moreover, the magnetic field decay also affects the thermal luminosity of a magnetar. Figure 6 shows the evolution of the thermal luminosity as computed via the thermal evolution equation,

$$c_V \frac{\partial T}{\partial t} = \nabla \cdot (\kappa \nabla T) - Q_\nu + \left(\frac{c}{4\pi}\right)^2 \frac{|\nabla \times \mathbf{B}|^2}{\sigma} \quad (5)$$

which is coupled to Eq. 3 not only by the dependence on the magnetic field and temperature of the transport coefficients (heat capacity c_V and conductivity κ , which is made a 3×3 tensor by the magnetic field), but also the last term on the RHS, which describes the Joule heating of the crust (and is the counterpart of the Ohmic dissipation term in the induction equation). Therefore, whereas the thermal evolution of ordinary NSs is mostly one of cooling, regulated by the neutrino emissivity term Q_ν (Yakovlev et al., 2001) and the emission of thermal radiation, in the case of magnetars field dissipation provides a substantial source of additional heating; this is reflected by the higher luminosity the curves in figure 6 can reach.

4.3 Modeling transient activity

As described in section 2, high energy, transient activity is the hallmark feature of magnetars. Owing to the large range of spatial and temporal scales involved, as well as the many different physical processes taking place, the efforts in modeling magnetar transients typically concentrate on either the description of magnetospheric processes or those happening within the star itself, with initial efforts to mathematically couple the two regions so far been able to tackle the long-term evolution only (Urbán et al., 2023); therefore, we will review in the following the two cases separately, even though in reality magnetar activity results from and is influenced by the dynamics in both regimes.

4.3.1 Transients & the Crust

One of the mechanisms often invoked as a trigger for transients is the release of elastic stress built up within the crust as a result the evolution of the magnetic field. The lattice structure of the crust, coupled with the enormous gravitational force, makes it extraordinarily resistant, as calculated by Chugunov and Horowitz (2010); still, ultra-strong fields, more so if tangled upon small scales by the Hall effect, can overcome the maximum yield. Several studies solving the magneto-thermal evolution in 2 or 3D (Perna and Pons, 2011; Dehman et al., 2020; De Grandis et al., 2020) and comparing the maximum yield from microphysical calculations to the magnetic stress tensor $M_{ij} = B_i B_j / 4\pi$ found that indeed in the early stages of the evolution of a strongly magnetized NS when the crust can fail due to the combined effect of field tangling and local Joule heating. Figure 7, right panel, shows an example of an early phase of a magnetothermal simulation in axial symmetry from Dehman et al. (2020), where the formation of localized hot, magnetized regions is apparent; the authors used these simulations to prove that young magnetars are indeed prone to develop crustal failures.

These violent events are often dubbed *starquakes*, even though the analogy with geophysical processes must be taken with care, as the strong gravity makes so that no cracks and voids are formed, but rather the crustal material starts flowing plastically (Lander and Gourgouliatos, 2019). The energy thus released can thereafter be converted to heat, possibly via Hall waves (Li et al., 2019), causing the formation of a hot spot. Field lines moving with the crust they are pinned to may also cause a reconfiguration of the magnetosphere.

The subsequent study of the cooling of the hotspot can be performed with a machinery akin to that used for secular cooling. This approach was first followed by Pons and Rea (2012), who found that the cooling timescales indeed match those observed for the evolution of magnetar outbursts, and highlighted the importance of neutrino emission from weak processes in the crust, which gets triggered above $\sim 3 \times 10^9$ K (Yakovlev et al., 2001), in regulating the peak luminosity that an outburst can reach; more detailed simulations (De Grandis et al., in preparation, Fig 8 top left panel) confirmed that neutrino emission from the outermost layers, in particular electron-positron weak annihilation and plasmon weak decay. This same result was confirmed by De Grandis et al. (2022) in a 3D setup, which also allowed to address the critical role of the field topology in determining the cooling properties of the outburst. In particular, the presence of a very tangled field makes so that the transport of heat to the source can happen in a complex pattern (figure 8, top right panel), suggesting that the values of the effective radii of hotspots as obtained by spectral fits must be regarded as effective ones, describing a more complicated underlying geometry in realistic cases.

4.3.2 Transients & the Magnetosphere

Due to their fast timescales and largely non-thermal nature, magnetar flares are associated with the field activity in the magnetosphere. In particular, they indicate that the field is not in a purely dipolar configuration (the only component that can be estimated from timing) but rather has a more tangled and variable topology. Whereas this implies the presence of currents in the magnetosphere in much greater abundance than for normal pulsars (Goldreich and Julian, 1969), the field is so strong that the magnetization parameter, i.e. the ratio of the magnetic pressure to the energy density of the plasma is still high, $B^2/4\pi\rho c^2 \gg 1$. This means that the magnetosphere can be treated to a good degree of approximation as a *force-free* plasma, namely one where

$$(\nabla \times \mathbf{B}) \times \mathbf{B} = \mathbf{0}. \quad (6)$$

In order to characterize the deviation of a field from a dipole, it is useful to define the *twist* angle associated to a field line as

$$\psi = \int_p^q \frac{B_\phi}{B r \sin \theta} d\ell = \int_p^q \frac{B_\phi}{B_\theta \sin \theta} d\theta \quad (7)$$

where the integral is taken along the field line itself, $\ell \parallel \mathbf{B}$, between the two points p and q where it touches the surface. Under the assumption of axial symmetry, i.e. constant twist ψ for all field lines, eq. 6 becomes known as the *Grad-Shafranov* equation (e.g. Pavan et al., 2009, and references therein); its solution, labeled by ψ , have been studied numerically, finding that stable configurations can be obtained for $\psi \lesssim 1$, whereas large twists $\psi \gg 1$ make the magnetosphere prone to instability and reconnection (Uzdensky, 2002; Carrasco et al., 2019). The shearing motion of the magnetar crust to which a line is pinned can increase the twist, triggering such unstable regime; this can directly be linked to flaring activity via the emission of Alfvén waves (e.g. Li et al., 2019, and references therein), as well as to outbursts via the heating of the crust by returning currents developing during the untwisting (Beloborodov, 2009).

5 Magnetars as Engines of Energetic Phenomena in the Universe

The vast majority of the known magnetars reside in the Milky Way or the nearby Magellanic Clouds. However, the enormous energy budget they store in rotational and magnetic power can in principle power transient events that can be detected from distances of cosmological relevance. The large efforts put in studying the transient Universe in the past years, allowed the discovery of a variety of new astrophysical classes and events, many of them proposed to be related with the formation of a magnetar and/or the typical large magnetar flares.

- **Compact binary mergers.** The recent discover of gravitational waves from a double NS binary (Abbott et al., 2017a,b) with the first electromagnetic counterpart as a short GRB and its afterglow, pointed to the production of a temporary magnetar as a viable explanation for the observed blue kilonova emission (Metzger et al., 2018).

- **Fast Radio Bursts (FRBs).** These are millisecond-long radio flares reaching us from distant Galaxies, which have also been suggested to be either connected to the formation of extra-Galactic magnetars, or being the radio counterparts of their energetic magnetar giant flares (Lieu, 2017; Beloborodov, 2017). These have gained particular traction after the *INTEGRAL* satellite detected an X-ray burst from the

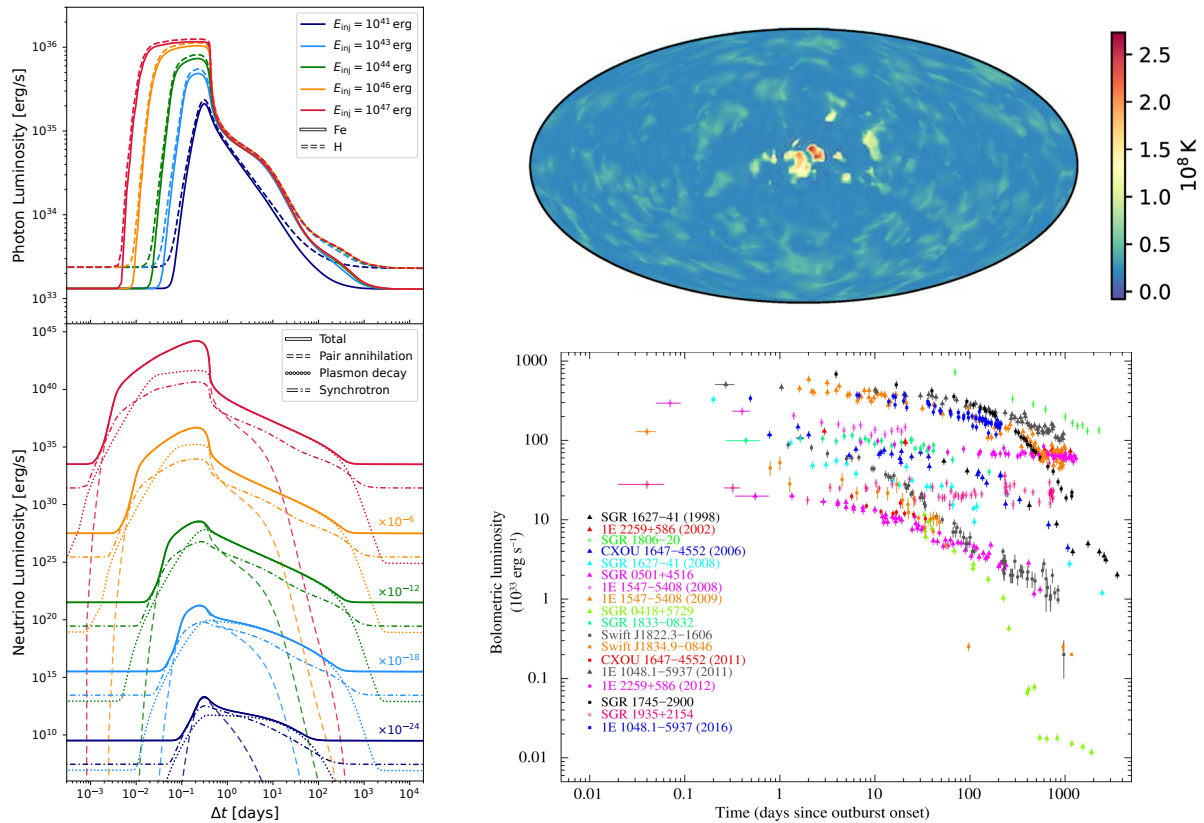


Fig. 8: (Left) Cooling of a 3 km hot feature in which a heat quantity H has been released over a short amount of time (10 h) in the outer crust; Δt indicates the time since the heating inception. The top panel shows the photon luminosity, in the case of a Fe (solid lines) or H (dashed lines) envelope model; the bottom one the corresponding neutrino luminosity, with its dominant channels (dashes lines: e^+e^- pair annihilation; dotted lines; plasmon decay; dot-dashed: weak synchrotron emission); from De Grandis et al., in preparation. (Top Right) Surface temperature of a NS with a tangled field during the cooling of a hotspot, which gets broken into several hot features by transport along field lines; from De Grandis et al. (2022). (Bottom Right) Evolution of the luminosity in the 18 magnetar outbursts recorded before 2018; from Coti Zelati et al. (2018a).

magnetar SGR 1935+2154 in temporal and spatial coincidence with an FRB (Mereghetti et al., 2020). This evidence strongly suggests that at least a fraction of the FRB population is indeed linked to magnetars.

- **Gamma-Ray Bursts (GRBs).** Several lines of evidence have been discovered that point to magnetars as proposed central engines of many long and short GRBs. In particular, their formation appears a good explanation for the GRB long-lived central engine activity (Metzger et al., 2011), for the multiple bursts of prompt emission in some GRBs (Bernardini, 2015), the extended emission in short GRBs (Gompertz et al., 2014), the X-ray plateau in both short and long GRBs (Rowlinson et al., 2013), and the recently discovered class of ultra-long gamma-ray bursts (Greiner et al., 2015).

- **Super-luminous supernovae (SLSNe).** Superluminous Supernovae are a class of particularly energetic SNe, characterized by an optical magnitude above -21 mag, corresponding to $L \gtrsim 10^{10} L_{\odot}$; this about 10 times the value for a normal SN Ia, and 100 times the one of a core collapse SN (see e.g. the review in Nicholl, 2021). Evidence is growing that the formation of magnetars powers also some super-luminous supernovae (SLSNe), their spin-down providing a delayed injection of energy (Dessart et al., 2012; Greiner et al., 2015).

6 Conclusions

Strongly magnetized neutron stars are unique laboratories to understand plasma and matter under extreme field regimes. The advent of X-ray satellites in the past few decades allowed the discovery of about 30 magnetars in our Galaxy. Magnetars are extremely variable sources, showing flares and outbursts on different timescales, and emitting from radio to soft γ -rays. The study of magnetars is therefore an active and expanding field, in which many mysteries remain to be solved. This chapter is too short to report exhaustively on the extensive past and present research on magnetars, and we acknowledge and apologize for the inevitable biases towards certain specific topics or publications.

Acknowledgments

NR and DDG are supported by the European Research Council (ERC) under the European Union's Horizon 2020 research and innovation programme (ERC Consolidator Grant "MAGNESIA" No. 817661) and from grant SGR2021-01269 from the Catalan Government. NR acknowledges support from the ESA Science Faculty Visitor program to ESTEC (funding reference ESA-SCI-E-LE-054), where most of this work has been carried out.

References

- Abbott BP, Abbott R, Abbott TD, Acernese and et al. (2017a), Oct. Multi-messenger Observations of a Binary Neutron Star Merger. *ApJ* 848 (2), L12. doi:10.3847/2041-8213/aa91c9. 1710.05833.
- Abbott BP and et al. (2017b), Oct. Gravitational Waves and Gamma-Rays from a Binary Neutron Star Merger: GW170817 and GRB 170817A. *ApJ* 848 (2), L13. doi:10.3847/2041-8213/aa920c. 1710.05834.
- Aguilera DN, Pons JA and Miralles JA (2008), Jul. 2D Cooling of magnetized neutron stars. *A&A* 486: 255–271. doi:10.1051/0004-6361:20078786.0710.0854.
- Aleksić J, Antonelli LA, Antoranz P, Asensio M, Barres de Almeida U, Barrio JA, Becerra González J, Bednarek W, Berger K, Bernardini E, Biland A, Blanch O, Bock RK, Boller A, Bonnoli G, Borla Tridon D, Bretz T, Carmona E, Carosi A, Colin P, Colombo E, Contreras JL, Cortina J, Cossio L, Covino S, Da Vela P, Dazzi F, De Angelis A, De Caneva G, De Cea del Pozo E, De Lotto B, Delgado Mendez C, Diago Ortega A, Doert M, Dominis Prester D, Dorner D, Doro M, Eisenacher D, Elsaesser D, Ferenc D, Fonseca MV, Font L, Fruck C, García López RJ, Garczarczyk M, Garrido Terrats D, Gaug M, Giavitto G, Godinović N, González Muñoz A, Gozzini SR, Hadamek A, Hadasch D, Häfner D, Herrero A, Hose J, Hrupec D, Huber B, Jankowski F, Jogler T, Kadenius V, Klepser S, Knoetig ML, Krähenbühl T, Krause J, Kushida J, La Barbera A, Lelas D, Leonardo E, Lewandowska N, Lindfors E, Lombardi S, López M, López-Coto R, López-Oramas A, Lorenz E, Makariev M, Maneva G, Mankuzhiyil N, Mannheim K, Maraschi L, Marcote B, Mariotti M, Martínez M, Mazin D, Meucci M, Miranda JM, Mirzoyan R, Moldón J, Moralejo A, Munar-Adrover P, Niedzwiecki A, Nieto D, Nilsson K, Nowak N, Orito R, Paiano S, Palatiello M, Paneque D, Paoletti R, Paredes JM, Partini S, Persic M, Pilia M, Pochon J, Prada F, Prada Moroni PG, Prandini E, Puljak I, Reichardt I, Reinthal R, Rhode W, Ribó M, Rico J, Rügamer S, Saggion A, Saito K, Saito TY, Salvati M, Satalecka K, Scalzotto V, Scapin V, Schultz C, Schweizer T, Shore SN, Sillanpää A, Sitarek J, Snidaric I, Sobczynska D, Spanier F, Spiro S, Stamatescu V, Stamera A, Steinke B, Storz J, Sun S, Surić T, Takalo L, Takami H, Tavecchio F, Temnikov P, Terzić T, Tesaro D, Teshima M, Tibolla O, Torres DF, Toyama T, Treves A, Uellenbeck M, Vogler P, Wagner RM, Weitzel Q, Zabalza V, Zandanel F, Zanin R, Rea N and Backes M (2013), Jan. Observations of the magnetars 4U 0142+61 and 1E 2259+586 with the MAGIC telescopes. *A&A* 549, A23. doi:10.1051/0004-6361/201220275. 1211.1173.
- An H, Kaspi VM, Archibald R, Bachetti M, Bhallerao V, Bellm EC, Beloborodov AM, Boggs SE, Chakrabarty D, Christensen FE, Craig WW, Dufour F, Forster K, Gotthelf EV, Grefenstette BW, Hailey CJ, Harrison FA, Hascoët R, Kitaguchi T, Kouveliotou C, Madsen KK, Mori K, Pivovarov MJ, Rana VR, Stern D, Tendulkar S, Tomsick JA, Vogel JK, Zhang WW and NuSTAR Team (2014), Mar. NuSTAR results and future plans for magnetar and rotation-powered pulsar observations. *Astronomische Nachrichten* 335: 280–284. doi:10.1002/asna.201312032. 1402.1079.
- Antonopoulou D, Haskell B and Espinoza CM (2022), Dec. Pulsar glitches: observations and physical interpretation. *Reports on Progress in Physics* 85 (12), 126901. doi:10.1088/1361-6633/ac9ced.
- Archibald RF, Burgay M, Lyutikov M, Kaspi VM, Esposito P, Israel G, Kerr M, Possenti A, Rea N, Sarkissian J, Scholz P and Tendulkar SP (2017), Nov. Magnetar-like X-Ray Bursts Suppress Pulsar Radio Emission. *ApJ* 849 (2), L20. doi:10.3847/2041-8213/aa9371. 1710.03718.
- Ascenzi S, Viganò D, Dehman C, Pons JA, Rea N and Perna R (2024), Jul. 3D code for MAgneto-Thermal evolution in Isolated Neutron Stars, MATINS: thermal evolution and light curves. *MNRAS* 533 (1): 201–224. doi:10.1093/mnras/stae1749. 2401.15711.
- Baring MG and Harding AK (2007), Apr. Resonant Compton upscattering in anomalous X-ray pulsars. *Ap&SS* 308: 109–118. doi:10.1007/s10509-007-9326-x. arXiv:astro-ph/0610382.
- Baring M, Wadiasingh Z, Gonthier PL, Harding AK and Hu K (2021), Jan., The Mysterious Magnetospheres of Magnetars (INVITED), High Energy Astrophysics in Southern Africa, pp. 36, 2012.10815.
- Barrère P, Guilet J, Reboul-Salze A, Raynaud R and Janka HT (2022), Dec. A new scenario for magnetar formation: Tayler-Spruit dynamo in a proto-neutron star spun up by fallback. *A&A* 668, A79. doi:10.1051/0004-6361/202244172. 2206.01269.
- Barrère P, Guilet J, Raynaud R and Reboul-Salze A (2024), Sep. 3D Tayler-Spruit dynamo in stably stratified rotating fluids: Application to protomagnetars. *arXiv e-prints*, arXiv:2407.01775doi:10.48550/arXiv.2407.01775. 2407.01775.
- Beloborodov AM (2009), Sep. Untwisting Magnetospheres of Neutron Stars. *ApJ* 703 (1): 1044–1060. doi:10.1088/0004-637X/703/1/1044.
- Beloborodov AM (2013), Jan. On the Mechanism of Hard X-Ray Emission from Magnetars. *ApJ* 762, 13. doi:10.1088/0004-637X/762/1/13. 1201.0664.
- Beloborodov AM (2017), Jul. A Flaring Magnetar in FRB 121102? *ApJ* 843 (2), L26. doi:10.3847/2041-8213/aa78f3. 1702.08644.
- Bernardini MG (2015), Sep. Gamma-ray bursts and magnetars: Observational signatures and predictions. *Journal of High Energy Astrophysics* 7: 64–72. doi:10.1016/j.jheap.2015.05.003.
- Bonanno A, Rezzolla L and Urpin V (2003), Oct. Mean-field dynamo action in protoneutron stars. *A&A* 410: L33–L36. doi:10.1051/0004-6361:20031459. astro-ph/0309783.
- Borghese A, Rea N, Turolla R, Rigoselli M, Alford JAJ, Gotthelf EV, Burgay M, Possenti A, Zane S, Coti Zelati F, Perna R, Esposito P, Mereghetti S, Viganò D, Tiengo A, Götz D, Ibrahim A, Israel GL, Pons J and Sathyaprakash R (2021), Jul. The X-ray evolution and geometry of the 2018 outburst of XTE J1810-197. *MNRAS* 504 (4): 5244–5257. doi:10.1093/mnras/stab1236. 2104.11083.
- Borghese A, Coti Zelati F, Israel GL, Pilia M, Burgay M, Trudu M, Zane S, Turolla R, Rea N, Esposito P, Mereghetti S, Tiengo A and Possenti A (2022), Oct. The first seven months of the 2020 X-ray outburst of the magnetar SGR J1935+2154. *MNRAS* 516 (1): 602–616. doi:10.1093/mnras/stac1314. 2205.04983.
- Camero A, Papitto A, Rea N, Viganò D, Pons JA, Tiengo A, Mereghetti S, Turolla R, Esposito P, Zane S, Israel GL and Götz D (2014), Mar. Quiescent state and outburst evolution of SGR 0501+4516. *MNRAS* 438 (4): 3291–3298. doi:10.1093/mnras/stt2432. 1312.4305.
- Camilo F, Ransom SM, Halpern JP, Reynolds J, Helfand DJ, Zimmerman N and Sarkissian J (2006), Aug. Transient pulsed radio emission from a magnetar. *Nature* 442: 892–895. doi:10.1038/nature04986. arXiv:astro-ph/0605429.
- Camilo F, Ransom SM, Halpern JP, Alford JAJ, Cognard I, Reynolds JE, Johnston S, Sarkissian J and van Straten W (2016), Apr. Radio Disappearance of the Magnetar XTE J1810-197 and Continued X-ray Timing. *ApJ* 820, 110. doi:10.3847/0004-637X/820/2/110. 1603.02170.
- Canuto V, Lodenquai J and Ruderman M (1971), May. Thomson scattering in a strong magnetic field. *Phys. Rev. D* 3: 2303–2308. doi:10.1103/PhysRevD.3.2303. <https://link.aps.org/doi/10.1103/PhysRevD.3.2303>.

- Carrasco F, Viganò D, Palenzuela C and Pons JA (2019), Mar. Triggering magnetar outbursts in 3D force-free simulations. *MNRAS* 484 (1): L124–L129. doi:10.1093/mnras/1slz016. 1901.08889.
- Chugunov AI and Horowitz CJ (2010), Sep. Breaking stress of neutron star crust. *MNRAS* 407 (1): L54–L58. doi:10.1111/j.1745-3933.2010.00903.x.
- Coti Zelati F, Rea N, Turolla R, Pons JA, Papitto A, Esposito P, Israel GL, Campana S, Zane S, Tiengo A, Mignani RP, Mereghetti S, Baganoff FK, Haggard D, Ponti G, Torres DF, Borghese A and Elfriz J (2017), Oct. Chandra monitoring of the Galactic Centre magnetar SGR J1745-2900 during the initial 3.5 years of outburst decay. *MNRAS* 471: 1819–1829. doi:10.1093/mnras/stx1700. 1707.01514.
- Coti Zelati F, Rea N, Pons JA, Campana S and Esposito P (2018a), Feb. Systematic study of magnetar outbursts. *MNRAS* 474 (1): 961–1017. doi:10.1093/mnras/stx2679.
- Coti Zelati F, Rea N, Pons JA, Campana S and Esposito P (2018b), Feb. Systematic study of magnetar outbursts. *MNRAS* 474: 961–1017. doi:10.1093/mnras/stx2679. 1710.04671.
- Coti Zelati F, Borghese A, Israel GL, Rea N, Esposito P, Pilia M, Burgay M, Possenti A, Corongiu A, Ridolfi A, Dehman C, Viganò D, Turolla R, Zane S, Tiengo A and Keane EF (2021), Feb. The New Magnetar SGR J1830-0645 in Outburst. *ApJ* 907 (2), L34. doi:10.3847/2041-8213/abda52. 2011.08653.
- De Grandis D, Turolla R, Wood TS, Zane S, Taverna R and Gourgouliatos KN (2020), Nov. Three-dimensional Modeling of the Magnetothermal Evolution of Neutron Stars: Method and Test Cases. *ApJ* 903 (1), 40. doi:10.3847/1538-4357/abb6f9. 2009.04331.
- De Grandis D, Turolla R, Taverna R, Lucchetta E, Wood TS and Zane S (2022), Sep. Three-dimensional Magnetothermal Simulations of Magnetar Outbursts. *ApJ* 936 (2), 99. doi:10.3847/1538-4357/ac8797. 2208.10178.
- Dehman C and Brandenburg A (2024), Aug. Reality of Inverse Cascading in Neutron Star Crusts. *arXiv e-prints*, arXiv:2408.08819doi:10.48550/arXiv.2408.08819. 2408.08819.
- Dehman C, Viganò D, Rea N, Pons JA, Perna R and Garcia-Garcia A (2020), Oct. On the Rate of Crustal Failures in Young Magnetars. *ApJ* 902 (2), L32. doi:10.3847/2041-8213/abbd9. 2010.00617.
- Dehman C, Viganò D, Ascenzi S, Pons JA and Rea N (2023), Aug. 3D evolution of neutron star magnetic fields from a realistic core-collapse turbulent topology. *MNRAS* 523 (4): 5198–5206. doi:10.1093/mnras/stad1773. 2305.06342.
- den Hartog PR, Kuiper L and Hermsen W (2008a), Oct. Detailed high-energy characteristics of AXP 1RXS J170849-400910. Probing the magnetosphere using INTEGRAL, RXTE, and XMM-Newton. *A&A* 489: 263–279. doi:10.1051/0004-6361:200809772. 0804.1641.
- den Hartog PR, Kuiper L, Hermsen W, Kaspi VM, Dib R, Knödseder J and Gavriil FP (2008b), Oct. Detailed high-energy characteristics of AXP 4U 0142+61. Multi-year observations with INTEGRAL, RXTE, XMM-Newton, and ASCA. *A&A* 489: 245–261. doi:10.1051/0004-6361:200809390. 0804.1640.
- Dessart L, Hillier DJ, Waldman R, Livne E and Blondin S (2012), Oct. Superluminous supernovae: ^{56}Ni power versus magnetar radiation. *MNRAS* 426 (1): L76–L80. doi:10.1111/j.1745-3933.2012.01329.x. 1208.1214.
- Dhillon VS, Marsh TR, Littlefair SP, Copperwheat CM, Hickman RDG, Kerry P, Levan AJ, Rea N, Savoury CDJ, Tanvir NR, Turolla R and Wiersema K (2011), Sep. The first observation of optical pulsations from a soft gamma repeater: SGR 0501+4516. *MNRAS* 416 (1): L16–L20. doi:10.1111/j.1745-3933.2011.01088.x. 1106.1355.
- Dib R and Kaspi VM (2014), Mar. 16 yr of RXTE Monitoring of Five Anomalous X-Ray Pulsars. *ApJ* 784, 37. doi:10.1088/0004-637X/784/1/37. 1401.3085.
- Dib R, Kaspi VM and Gavriil FP (2008), Feb. Glitches in Anomalous X-Ray Pulsars. *ApJ* 673: 1044–1061. doi:10.1086/524653.
- Dib R, Kaspi VM, Scholz P and Gavriil FP (2012), Mar. RXTE Observations of Anomalous X-Ray Pulsar 1E 1547.0-5408 during and after its 2008 and 2009 Outbursts. *ApJ* 748 (1), 3. doi:10.1088/0004-637X/748/1/3. 1201.2668.
- Duncan RC and Thompson C (1992), Jun. Formation of very strongly magnetized neutron stars - Implications for gamma-ray bursts. *ApJ* 392: L9–L13.
- Enoto T, Shibata S, Kitaguchi T, Suwa Y, Uchide T, Nishioka H, Kisaka S, Nakano T, Murakami H and Makishima K (2017), Jul. Magnetar Broadband X-Ray Spectra Correlated with Magnetic Fields: Suzaku Archive of SGRs and AXPs Combined with NuSTAR, Swift, and RXTE. *ApJS* 231, 8. doi:10.3847/1538-4365/aa6f0a. 1704.07018.
- Enoto T, Ng M, Hu CP, Güver T, Jaisawal GK, O'Connor B, Göğüş E, Lien A, Kisaka S, Wadiasingh Z, Majid WA, Pearlman AB, Arzoumanian Z, Bansal K, Blumer H, Chakrabarty D, Gendreau K, Ho WCG, Kouveliotou C, Ray PS, Strohmayer TE, Younes G, Palmer DM, Sakamoto T, Akahori T and Eie S (2021), oct. A month of monitoring the new magnetar swift j1555.2-5402 during an x-ray outburst. *The Astrophysical Journal Letters* 920 (1): L4. doi:10.3847/2041-8213/ac2665. <https://dx.doi.org/10.3847/2041-8213/ac2665>.
- Esposito P, Tiengo A, Mereghetti S, Israel GL, De Luca A, Götz D, Rea N, Turolla R and Zane S (2009), Jan. Xmm-Newton Discovery of 2.6 s Pulsations in the Soft Gamma-Ray Repeater SGR 1627-41. *ApJ* 690: L105–L109. doi:10.1088/0004-637X/690/2/L105.
- Esposito P, Israel GL, Turolla R, Mattana F, Tiengo A, Possenti A, Zane S, Rea N, Burgay M, Götz D, Mereghetti S, Stella L, Wieringa MH, Sarkissian JM, Enoto T, Romano P, Sakamoto T, Nakagawa YE, Makishima K, Nakazawa K, Nishioka H and François-Martin C (2011), Sep. Long-term spectral and timing properties of the soft gamma-ray repeater SGR 1833-0832 and detection of extended X-ray emission around the radio pulsar PSR B1830-08. *MNRAS* 416: 205–215. doi:10.1111/j.1365-2966.2011.19022.x. 1105.1323.
- Esposito P, Motta SE, Pintore F, Zampieri L and Tomasella L (2013), Jan. Swift observations of the ultraluminous X-ray source XMMU J004243.6+412519 in M31. *MNRAS* 428: 2480–2488. doi:10.1093/mnras/sts248. 1210.5099.
- Esposito P, Rea N, Borghese A, Coti Zelati F, Viganò D, Israel GL, Tiengo A, Ridolfi A, Possenti A, Burgay M, Götz D, Pintore F, Stella L, Dehman C, Ronchi M, Campana S, Garcia-Garcia A, Graber V, Mereghetti S, Perna R, Rodríguez Castillo GA, Turolla R and Zane S (2020), Jun. A Very Young Radio-loud Magnetar. *ApJ* 896 (2), L30. doi:10.3847/2041-8213/ab9742. 2004.04083.
- Esposito P, Rea N and Israel GL (2021), Jan., Magnetars: A Short Review and Some Sparse Considerations, Belloni TM, Méndez M and Zhang C, (Eds.), *Astrophysics and Space Science Library, Astrophysics and Space Science Library*, 461, 97–142, 1803.05716.
- Fernández R and Thompson C (2007), May. Resonant Cyclotron Scattering in Three Dimensions and the Quiescent Nonthermal X-ray Emission of Magnetars. *ApJ* 660: 615–640. doi:10.1086/511810. arXiv:astro-ph/0608281.
- Ferrario L and Wickramasinghe D (2006), Apr. Modelling of isolated radio pulsars and magnetars on the fossil field hypothesis. *MNRAS* 367 (3): 1323–1328. doi:10.1111/j.1365-2966.2006.10058.x. astro-ph/0601258.
- Flowers EG, Ruderman MA, Lee JF, Sutherland PG, Hillebrandt W and Mueller E (1977), Jul. Variational calculation of ground-state energy of iron atoms and condensed matter in strong magnetic fields. *ApJ* 215: 291–301. doi:10.1086/155358.
- Fushiki I, Gudmundsson EH, Pethick CJ and Yngvason J (1992), May. Matter in a magnetic field in the Thomas-Fermi and related theories. *Annals of Physics* 216 (1): 29–72. doi:10.1016/0003-4916(92)90041-9.
- Gavriil FP, Kaspi VM and Woods PM (2002), Sep. Magnetar-like X-ray bursts from an anomalous X-ray pulsar. *Nature* 419 (6903): 142–144. doi:10.1038/nature01011. astro-ph/0209202.
- Gold T (1968), May. Rotating Neutron Stars as the Origin of the Pulsating Radio Sources. *Nature* 218 (5143): 731–732. doi:10.1038/218731a0.
- Goldreich P and Julian WH (1969), Aug. Pulsar Electrodynamics. *ApJ* 157: 869. doi:10.1086/150119.
- Goldreich P and Reisenegger A (1992), Aug. Magnetic Field Decay in Isolated Neutron Stars. *ApJ* 395: 250. doi:10.1086/171646.

- Gompertz BP, O'Brien PT and Wynn GA (2014), Feb. Magnetar powered GRBs: explaining the extended emission and X-ray plateau of short GRB light curves. *MNRAS* 438 (1): 240–250. doi:10.1093/mnras/stt2165. 1311.1505.
- Götz D, Mereghetti S, Tiengo A and Esposito P (2006), Apr. Magnetars as persistent hard X-ray sources: INTEGRAL discovery of a hard tail in SGR 1900+14. *A&A* 449: L31–L34. doi:10.1051/0004-6361:20064870.
- Götz D, Rea N, Israel GL, Zane S, Esposito P, Gotthelf EV, Mereghetti S, Tiengo A and Turolla R (2007), Nov. Long term hard X-ray variability of the anomalous X-ray pulsar 1RXS J170849.0-400910 discovered with INTEGRAL. *A&A* 475: 317–321. doi:10.1051/0004-6361:20078291. arXiv:0709.3712.
- Gourgouliatos KN, Wood TS and Hollerbach R (2016), Apr. Magnetic field evolution in magnetar crusts through three-dimensional simulations. *Proceedings of the National Academy of Science* 113 (15): 3944–3949. doi:10.1073/pnas.1522363113. 1604.01399.
- Greiner J, Mazzali PA, Kann DA, Krühler T, Pian E, Prentice S, Olivares E. F, Rossi A, Klose S, Taubenberger S, Knust F, Afonso PMJ, Ashall C, Bolmer J, Delvaux C, Diehl R, Elliott J, Filgas R, Fynbo JPU, Graham JF, Guelbenzu AN, Kobayashi S, Leloudas G, Savaglio S, Schady P, Schmidl S, Schweyer T, Sudilovsky V, Tanga M, Urdike AC, van Eerten H and Varela K (2015), Jul. A very luminous magnetar-powered supernova associated with an ultra-long γ -ray burst. *Nature* 523 (7559): 189–192. doi:10.1038/nature14579. 1509.03279.
- Hare J, Pavlov GG, Posselt B, Kargaltsev O, Temim T and Chen S (2024), Sep. Probing the Spectrum of the Magnetar 4U 0142+61 with JWST. *ApJ* 972 (2), 176. doi:10.3847/1538-4357/ad5ce5. 2405.03947.
- Hulleman F, van Kerkwijk MH and Kulkarni SR (2004), Mar. The Anomalous X-ray Pulsar 4U 0142+61: Variability in the infrared and a spectral break in the optical. *A&A* 416: 1037–1045. doi:10.1051/0004-6361:20031756.
- Ibrahim AI, Markwardt CB, Swank JH, Ransom S, Roberts M, Kaspi V, Woods PM, Safi-Harb S, Balman S, Parke WC, Kouveliotou C, Hurley K and Cline T (2004a), Jul. Discovery of a Transient Magnetar: XTE J1810-197. *ApJ* 609 (1): L21–L24. doi:10.1086/422636. astro-ph/0310665.
- Ibrahim AI, Markwardt CB, Swank JH, Ransom S, Roberts M, Kaspi V, Woods PM, Safi-Harb S, Balman S, Parke WC, Kouveliotou C, Hurley K and Cline T (2004b), Jul. Discovery of a Transient Magnetar: XTE J1810-197. *ApJ* 609: L21–L24. doi:10.1086/422636. astro-ph/0310665.
- Ibrahim AY, Borghese A, Coti Zelati F, Parent E, Marino A, Ould-Boukattine OS, Rea N, Ascenzi S, Pacholski DP, Mereghetti S, Israel GL, Tiengo A, Possenti A, Burgay M, Turolla R, Zane S, Esposito P, Götz D, Campana S, Kirsten F, Gawroński MP and Hessels JWC (2024), Apr. An X-Ray and Radio View of the 2022 Reactivation of the Magnetar SGR J1935+2154. *ApJ* 965 (1), 87. doi:10.3847/1538-4357/ad293b. 2402.08596.
- Igoshev AP, Hollerbach R, Wood T and Gourgouliatos KN (2020), Oct. Strong toroidal magnetic fields required by quiescent X-ray emission of magnetars. *Nature Astronomy* doi:10.1038/s41550-020-01220-z.
- Israel GL, Romano P, Mangano V, Dall'Osso S, Chincarini G, Stella L, Campana S, Belloni T, Tagliaferri G, Blustin AJ, Sakamoto T, Hurley K, Zane S, Moretti A, Palmer D, Guidorzi C, Burrows DN, Gehrels N and Krimm HA (2008), Oct. A Swift Gaze into the 2006 March 29 Burst Forest of SGR 1900+14. *ApJ* 685: 1114–1128. doi:10.1086/590486. 0805.3919.
- Israel GL, Esposito P, Rea N, Coti Zelati F, Tiengo A, Campana S, Mereghetti S, Rodriguez Castillo GA, Götz D, Burgay M, Possenti A, Zane S, Turolla R, Perna R, Cannizzaro G and Pons J (2016), Apr. The discovery, monitoring and environment of SGR J1935+2154. *MNRAS* 457 (4): 3448–3456. doi:10.1093/mnras/stw008. 1601.00347.
- Jones PB (1986), Oct. Pair creation in radio pulsars : the return-current mode changes and normal-null transitions. *MNRAS* 222: 577–591. doi:10.1093/mnras/222.3.577.
- Kaspi VM and Beloborodov AM (2017), Aug. Magnetars. *ARA&A* 55 (1): 261–301. doi:10.1146/annurev-astro-081915-023329. 1703.00068.
- Kaspi VM, Gavriil FP, Woods PM, Jensen JB, Roberts MSE and Chakrabarty D (2003), May. A Major Soft Gamma Repeater-like Outburst and Rotation Glitch in the No-longer-so-anomalous X-Ray Pulsar 1E 2259+586. *ApJ* 588: L93–L96.
- Kern B and Martin C (2002), May. Optical pulsations from the anomalous X-ray pulsar 4U0142+61. *Nature* 417 (6888): 527–529. doi:10.1038/417527a.
- Kouveliotou C, Dieters S, Strohmayer T, van Paradijs J, Fishman GJ, Meegan CA, Hurley K, Kommers J, Smith I, Frail D and Murakami T (1998), May. An X-ray pulsar with a superstrong magnetic field in the soft γ -ray repeater SGR1806 - 20. *Nature* 393 (6682): 235–237. doi:10.1038/30410.
- Kouveliotou C, Strohmayer T, Hurley K, van Paradijs J, Finger MH, Dieters S, Woods P, Thompson C and Duncan RC (1999), Jan. Discovery of a Magnetar Associated with the Soft Gamma Repeater SGR 1900+14. *ApJ* 510 (2): L115–L118. doi:10.1086/311813. astro-ph/9809140.
- Kuiper L, Hermsen W and Mendez M (2004), Oct. Discovery of Hard Nonthermal Pulsed X-Ray Emission from the Anomalous X-Ray Pulsar 1E 1841-045. *ApJ* 613: 1173–1178. doi:10.1086/423129.
- Kuiper L, Hermsen W, den Hartog PR and Collmar W (2006), Jul. Discovery of Luminous Pulsed Hard X-Ray Emission from Anomalous X-Ray Pulsars 1RXS J1708-4009, 4U 0142+61, and 1E 2259+586 by INTEGRAL and RXTE. *ApJ* 645: 556–575. doi:10.1086/504317. astro-ph/0603467.
- Lander SK and Gourgouliatos KN (2019), Jul. Magnetic-field evolution in a plastically failing neutron-star crust. *MNRAS* 486 (3): 4130–4143. doi:10.1093/mnras/stz1042.
- Laros JG, Fenimore EE, Fikani MM, Klebesadel RW and Barat C (1986), Jul. The soft γ -ray burst GB790107. *Nature* 322 (6075): 152–153. doi:10.1038/322152a0.
- Levin L, Bailes M, Bates S, Bhat NDR, Burgay M, Burke-Spolaor S, D'Amico N, Johnston S, Keith M, Kramer M, Milia S, Possenti A, Rea N, Stappers B and van Straten W (2010), Sep. A Radio-loud Magnetar in X-ray Quiescence. *ApJ* 721: L33–L37. doi:10.1088/2041-8205/721/1/L33. 1007.1052.
- Li J, Rea N, Torres DF and de Oña-Wilhelmi E (2017), Jan. Gamma-ray Upper Limits on Magnetars with Six Years of Fermi-LAT Observations. *ApJ* 835, 30. doi:10.3847/1538-4357/835/1/30. 1607.03778.
- Li X, Zrake J and Beloborodov AM (2019), Aug. Dissipation of Alfvén Waves in Relativistic Magnetospheres of Magnetars. *ApJ* 881 (1), 13. doi:10.3847/1538-4357/ab2a03. 1810.10493.
- Lieu R (2017), Jan. Are Fast Radio Bursts the Birthmark of Magnetars? *ApJ* 834 (2), 199. doi:10.3847/1538-4357/834/2/199. 1611.03094.
- Lytikov M and Gavriil FP (2006), May. Resonant cyclotron scattering and Comptonization in neutron star magnetospheres. *MNRAS* 368 (2): 690–706. doi:10.1111/j.1365-2966.2006.10140.x. astro-ph/0507557.
- Maan Y, Surnis MP, Chandra Joshi B and Bagchi M (2022), May. Magnetar XTE J1810-197: Spectro-temporal Evolution of Average Radio Emission. *ApJ* 931 (1), 67. doi:10.3847/1538-4357/ac68f1. 2201.13006.
- Makarenko EI, Igoshev AP and Kholtygin AF (2021), Jul. Testing the fossil field hypothesis: could strongly magnetized OB stars produce all known magnetars? *MNRAS* 504 (4): 5813–5828. doi:10.1093/mnras/stab1175. 2104.10579.
- Masada Y, Takiwaki T and Kotake K (2022), Jan. Convection and Dynamo in Newly Born Neutron Stars. *ApJ* 924 (2), 75. doi:10.3847/1538-4357/ac34f6. 2001.08452.
- Mazets EP, Golenetskii SV, Il'Inskii VN, Panov VN, Aptekar' RL, Gur'yan YA, Sokolov IA, Sokolova ZY and Kharitonova TV (1979), Apr. A flaring x-ray pulsar in Dorado. *Soviet Astronomy Letters* 5: 163.
- Medin Z and Lai D (2006), Dec. Density-functional-theory calculations of matter in strong magnetic fields. II. Infinite chains and condensed

- matter. *Phys. Rev. A* 74 (6), 062508. doi:10.1103/PhysRevA.74.062508. astro-ph/0607277.
- Mereghetti S and Stella L (1995), Mar. The very low mass X-ray binary pulsars: A new class of sources? *ApJ* 442: L17–L20.
- Mereghetti S, Pons JA and Melatos A (2018), Magnetars: Properties, Origin and Evolution, Beskin VS, Balogh A, Falanga M, Lyutikov M, Mereghetti S, Piran T and Treumann RA, (Eds.), *The Strongest Magnetic Fields in the Universe*, 54, 321–344.
- Mereghetti S, Savchenko V, Ferrigno C, Götz D, Rigoselli M, Tiengo A, Bazzano A, Bozzo E, Coleiro A, Courvoisier T, Doyle M, Goldwurm A, Hanlon L, Jourdain E, von Kienlin A, Lutovinov A, Martin-Carrillo A, Molokov S, Natalucci L, Onori F, Panessa F, Rodi J, Rodriguez J, Sánchez-Fernández C, Sunyaev R and Ubertini P (2020), Aug. INTEGRAL Discovery of a Burst with Associated Radio Emission from the Magnetar SGR 1935+2154. *ApJ* 898 (2), L29. doi:10.3847/2041-8213/aba2cf. 2005.06335.
- Mereghetti S, Rigoselli M, Salvaterra R, Pacholski DP, Rodi JC, Gotz D, Arrighoni E, D'Avanzo P, Adami C, Bazzano A, Bozzo E, Brivio R, Campana S, Cappellaro E, Chenevez J, De Luise F, Ducci L, Esposito P, Ferrigno C, Ferro M, Israel GL, Le Floc'h E, Martin-Carrillo A, Onori F, Rea N, Reguitti A, Savchenko V, Souami D, Tartaglia L, Thuillot W, Tiengo A, Tomasella L, Topinka M, Turpin D and Ubertini P (2024), May. A magnetar giant flare in the nearby starburst galaxy M82. *Nature* 629 (8010): 58–61. doi:10.1038/s41586-024-07285-4. 2312.14645.
- Metzger BD, Giannios D, Thompson TA, Bucciantini N and Quataert E (2011), May. The protomagnetar model for gamma-ray bursts. *MNRAS* 413 (3): 2031–2056. doi:10.1111/j.1365-2966.2011.18280.x. 1012.0001.
- Metzger BD, Thompson TA and Quataert E (2018), Apr. A Magnetar Origin for the Kilonova Ejecta in GW170817. *ApJ* 856 (2), 101. doi:10.3847/1538-4357/aab095. 1801.04286.
- Neuhauser D, Koonin SE and Langanke K (1987), Nov. Structure of matter in strong magnetic fields. *Phys. Rev. A* 36 (9): 4163–4175. doi:10.1103/PhysRevA.36.4163.
- Nicholl M (2021), Oct. Superluminous supernovae: an explosive decade. *Astronomy and Geophysics* 62 (5): 5.34–5.42. doi:10.1093/astrogeo/atab092. 2109.08697.
- Nobili L, Turolla R and Zane S (2008), May. X-ray spectra from magnetar candidates - I. Monte Carlo simulations in the non-relativistic regime. *MNRAS* 386: 1527–1542. doi:10.1111/j.1365-2966.2008.13125.x. 0802.2647.
- Obergaulinger M, Cerdá-Durán P, Müller E and Aloy MA (2009), Apr. Semi-global simulations of the magneto-rotational instability in core collapse supernovae. *A&A* 498 (1): 241–271. doi:10.1051/0004-6361/200811323. 0811.1652.
- Olausen SA and Kaspi VM (2014), May. The McGill Magnetar Catalog. *ApJS* 212, 6. doi:10.1088/0067-0049/212/1/6. 1309.4167.
- Palmer DM, Barthelmy S, Gehrels N, Kippen RM, Cayton T, Kouveliotou C, Eichler D, Wijers RAMJ, Woods PM, Granot J, Lyubarsky YE, Ramirez-Ruiz E, Barbier L, Chester M, Cummings J, Fenimore EE, Finger MH, Gaensler BM, Hullinger D, Krimm H, Markwardt CB, Nousek JA, Parsons A, Patel S, Sakamoto T, Sato G, Suzuki M and Tueller J (2005), Apr. A giant γ -ray flare from the magnetar SGR 1806 - 20. *Nature* 434: 1107–1109. doi:10.1038/nature03525.
- Pavan L, Turolla R, Zane S and Nobili L (2009), May. Topology of magnetars external field - I. Axially symmetric fields. *MNRAS* 395 (2): 753–763. doi:10.1111/j.1365-2966.2009.14600.x. 0902.0720.
- Perna R and Pons JA (2011), Feb. A Unified Model of the Magnetar and Radio Pulsar Bursting Phenomenology. *ApJ* 727 (2), L51. doi:10.1088/2041-8205/727/2/L51. 1101.1098.
- Pons JA and Rea N (2012), May. Modeling Magnetar Outbursts: Flux Enhancements and the Connection with Short Bursts and Glitches. *ApJ* 750 (1), L6. doi:10.1088/2041-8205/750/1/L6.
- Pons JA and Viganò D (2019), Dec. Magnetic, thermal and rotational evolution of isolated neutron stars. *Living Reviews in Computational Astrophysics* 5 (1). ISSN 2365-0524. doi:10.1007/s41115-019-0006-7. <http://dx.doi.org/10.1007/s41115-019-0006-7>.
- Pons JA, Viganò D and Rea N (2013), Jul. A highly resistive layer within the crust of X-ray pulsars limits their spin periods. *Nature Physics* 9 (7): 431–434. doi:10.1038/nphys2640. 1304.6546.
- Potekhin AY and Chabrier G (2013), Feb. Equation of state for magnetized Coulomb plasmas. *A&A* 550, A43. doi:10.1051/0004-6361/201220082. 1212.3405.
- Potekhin AY, Pons JA and Page D (2015), Oct. Neutron Stars—Cooling and Transport. *Space Science Reviews* 191: 239–291.
- Rea N and Esposito P (2011), Magnetar outbursts: an observational review, Torres DF and Rea N, (Eds.), *High-Energy Emission from Pulsars and their Systems. Proceedings of the First Session of the Sant Cugat Forum on Astrophysics, Astrophysics and Space Science Proceedings*, Springer, Heidelberg, 247–273.
- Rea N, Testa V, Israel GL, Mereghetti S, Perna R, Stella L, Tiengo A, Mangano V, Oosterbroek T, Mignani R, Lo Curto G, Campana S and Covino S (2004), Oct. Correlated Infrared and X-ray variability of the transient Anomalous X-ray Pulsar XTE J1810-197. *A&A* 425: L5–L8. doi:10.1051/0004-6361:200400052. arXiv:astro-ph/0408087.
- Rea N, Zane S, Turolla R, Lyutikov M and Götz D (2008), Oct. Resonant Cyclotron Scattering in Magnetars' Emission. *ApJ* 686: 1245–1260. doi:10.1086/591264. 0802.1923.
- Rea N, Israel GL, Turolla R, Esposito P, Mereghetti S, Götz D, Zane S, Tiengo A, Hurley K, Feroci M, Still M, Yershov V, Winkler C, Perna R, Bernardini F, Ubertini P, Stella L, Campana S, van der Klis M and Woods P (2009), Jul. The first outburst of the new magnetar candidate SGR0501+4516. *MNRAS* 396: 2419–2432. doi:10.1111/j.1365-2966.2009.14920.x. 0904.2413.
- Rea N, Esposito P, Turolla R, Israel GL, Zane S, Stella L, Mereghetti S, Tiengo A, Götz D, Göğüş E and Kouveliotou C (2010), Nov. A Low-Magnetic-Field Soft Gamma Repeater. *Science* 330: 944. doi:10.1126/science.1196088. 1010.2781.
- Rea N, Israel GL, Esposito P, Pons JA, Camero-Arranz A, Mignani RP, Turolla R, Zane S, Burgay M, Possenti A, Campana S, Enoto T, Gehrels N, Göğüş E, Götz D, Kouveliotou C, Makishima K, Mereghetti S, Oates SR, Palmer DM, Perna R, Stella L and Tiengo A (2012a), Jul. A New Low Magnetic Field Magnetar: The 2011 Outburst of Swift J1822.3-1606. *ApJ* 754 (1), 27. doi:10.1088/0004-637X/754/1/27.
- Rea N, Pons JA, Torres DF and Turolla R (2012b), Mar. The Fundamental Plane for Radio Magnetars. *ApJ* 748, L12. doi:10.1088/2041-8205/748/1/L12. 1202.3069.
- Rea N, Israel GL, Pons JA, Turolla R, Viganò D, Zane S, Esposito P, Perna R, Papitto A, Terreran G, Tiengo A, Salvetti D, Girart JM, Palau A, Possenti A, Burgay M, Göğüş E, Caliendo GA, Kouveliotou C, Götz D, Mignani RP, Ratti E and Stella L (2013), Jun. The Outburst Decay of the Low Magnetic Field Magnetar SGR 0418+5729. *ApJ* 770, 65. doi:10.1088/0004-637X/770/1/65. 1303.5579.
- Rea N, Viganò D, Israel GL, Pons JA and Torres DF (2014), Jan. 3XMM J185246.6+003317: Another Low Magnetic Field Magnetar. *ApJ* 781 (1), L17. doi:10.1088/2041-8205/781/1/L17. 1311.3091.
- Rea N, Borghese A, Esposito P, Coti Zelati F, Bachetti M, Israel GL and De Luca A (2016), Sep. Magnetar-like Activity from the Central Compact Object in the SNR RCW103. *ApJ* 828, L13. doi:10.3847/2041-8205/828/1/L13. 1607.04107.
- Reboul-Salze A, Guilet J, Raynaud R and Bugli M (2021), Jan. A global model of the magnetorotational instability in proton-neutron stars. *A&A* 645, A109. doi:10.1051/0004-6361/202038369. 2005.03567.
- Reboul-Salze A, Guilet J, Raynaud R and Bugli M (2022), Nov. MRI-driven $\alpha\Omega$ dynamos in proton-neutron stars. *A&A* 667, A94. doi:10.1051/0004-6361/202142368. 2111.02148.
- Rodríguez Castillo GA, Israel GL, Esposito P, Pons JA, Rea N, Turolla R, Viganò D and Zane S (2014), Jun. Pulse phase-coherent timing and spectroscopy of CXOU J164710.2-45521 outbursts. *MNRAS* 441 (2): 1305–1316. doi:10.1093/mnras/stu603. 1403.7165.

- Rodríguez Castillo GA, Israel GL, Tiengo A, Salvetti D, Turolla R, Zane S, Rea N, Esposito P, Mereghetti S, Perna R, Stella L, Pons JA, Campana S, Götz D and Motta S (2016), Mar. The outburst decay of the low magnetic field magnetar SWIFT J1822.3-1606: phase-resolved analysis and evidence for a variable cyclotron feature. *MNRAS* 456: 4145–4155. doi:10.1093/mnras/stv2490. 1510.09157.
- Rowlinson A, O'Brien PT, Metzger BD, Tanvir NR and Levan AJ (2013), Apr. Signatures of magnetar central engines in short GRB light curves. *MNRAS* 430 (2): 1061–1087. doi:10.1093/mnras/sts683. 1301.0629.
- Ruderman M (1974), Jan., Matter in Superstrong Magnetic Fields, Hansen CJ, (Ed.), *Physics of Dense Matter*, IAU Symposium, 53, pp. 117.
- Tam CR, Kaspi VM, van Kerkwijk MH and Durant M (2004), Dec. Correlated Infrared and X-Ray Flux Changes Following the 2002 June Outburst of the Anomalous X-Ray Pulsar 1E 2259+586. *ApJ* 617 (1): L53–L56. doi:10.1086/426963. astro-ph/0409351.
- Taverna R and Turolla R (2024), Feb. X-ray Polarization from Magnetar Sources. *Galaxies* 12 (1), 6. doi:10.3390/galaxies12010006. 2402.05622.
- Taverna R, Turolla R, Muleri F, Heyl J, Zane S, Baldini L, González-Caniulef D, Bachetti M, Rankin J, Caiazzo I, Di Lalla N, Doroshenko V, Errando M, Gau E, Kirmizibayrak D, Krawczynski H, Negro M, Ng M, Omodei N, Possenti A, Tamagawa T, Uchiyama K, Weisskopf MC, Agudo I, Antonelli LA, Baumgartner WH, Bellazzini R, Bianchi S, Bongiorno SD, Bonino R, Brez A, Bucciantini N, Capitanio F, Castellano S, Cavazzuti E, Ciprini S, Costa E, De Rosa A, Del Monte E, Di Gesù L, Di Marco A, Donnarumma I, Dovčiak M, Ehler SR, Enoto T, Evangelista Y, Fabiani S, Ferrazzoli R, Garcia JA, Gunji S, Hayashida K, Iwakiri W, Jorstad SG, Karas V, Kitaguchi T, Kolodziejczak JJ, La Monaca F, Latronico L, Liodakis I, Maldera S, Manfreda A, Marin F, Marinucci A, Marscher AP, Marshall HL, Matt G, Mitsuishi I, Mizuno T, Ng SCY, O'Dell SL, Oppedisano C, Papitto A, Pavlov GG, Peirson AL, Perri M, Pesce-Rollins M, Pilia M, Poutanen J, Puccetti S, Ramsey BD, Ratheesh A, Romani RW, Sgrò C, Slane P, Soffitta P, Spandre G, Tavecchio F, Tawara Y, Tennant AF, Thomas NE, Tombesi F, Trois A, Tsygankov SS, Vink J, Wu K and Xie F (2022), Nov. Polarized x-rays from a magnetar. *Science* 378 (6620): 646–650. doi:10.1126/science.add0080. 2205.08898.
- Thompson C and Duncan RC (1993), Jan., X-ray emission from neutron stars with supercritical magnetic fields: a model for the soft gamma repeaters., Friedlander N, Gehrels N and Macomb DJ, (Eds.), *Compton Gamma-ray Observatory*, American Institute of Physics Conference Series, 280, 1085–1089.
- Tiengo A, Esposito P, Mereghetti S, Turolla R, Nobili L, Gastaldello F, Götz D, Israel GL, Rea N, Stella L, Zane S and Bignami GF (2013), Aug. *Nature* 500 (7462): 312–314. doi:10.1038/nature12386.
- Turolla R, Zane S and Drake JJ (2004), Mar. Bare Quark Stars or Naked Neutron Stars? The Case of RX J1856.5-3754. *ApJ* 603 (1): 265–282. doi:10.1086/379113. astro-ph/0308326.
- Turolla R, Zane S and Watts AL (2015a), Nov. Magnetars: the physics behind observations. A review. *Reports on Progress in Physics* 78 (11), 116901. doi:10.1088/0034-4885/78/11/116901.
- Turolla R, Zane S and Watts AL (2015b). Magnetars: the physics behind observations. a review. *Reports on Progress in Physics* 78: 116901. <http://stacks.iop.org/0034-4885/78/i=11/a=116901>.
- Urbán JF, Stefanou P, Dehman C and Pons JA (2023), Sep. Modelling force-free neutron star magnetospheres using physics-informed neural networks. *MNRAS* 524 (1): 32–42. doi:10.1093/mnras/stad1810. 2303.11968.
- Uzdensky DA (2002), Aug. Shear-driven Field-Line Opening and the Loss of a Force-free Magnetostatic Equilibrium. *ApJ* 574 (2): 1011–1020. doi:10.1086/341119. astro-ph/0206061.
- Viganò D, Rea N, Pons JA, Perna R, Aguilera DN and Miralles JA (2013), Sep. Unifying the observational diversity of isolated neutron stars via magneto-thermal evolution models. *MNRAS* 434: 123–141. doi:10.1093/mnras/stt1008. 1306.2156.
- Wadiasingh Z, Baring MG, Gonthier PL and Harding AK (2018), Feb. Resonant Inverse Compton Scattering Spectra from Highly Magnetized Neutron Stars. *ApJ* 854 (2), 98. doi:10.3847/1538-4357/aaa460. 1712.09643.
- White CJ, Burrows A, Coleman MSB and Vartanyan D (2022), Feb. On the Origin of Pulsar and Magnetar Magnetic Fields. *ApJ* 926 (2), 111. doi:10.3847/1538-4357/ac4507. 2111.01814.
- Wiebicke HJ and Geppert U (1996), May. Amplification of neutron star magnetic fields by thermoelectric effects. VI. Analytical approach. *A&A* 309: 203–212.
- Wood TS, Hollerbach R and Lyutikov M (2014), May. Density-shear instability in electron magneto-hydrodynamics. *Physics of Plasmas* 21 (5), 052110. doi:10.1063/1.4879810.
- Woods PM, Kouveliotou C, Gavriil FP, Kaspi VM, Roberts MSE, Ibrahim A, Markwardt CB, Swank JH and Finger MH (2005), Aug. X-Ray Bursts from the Transient Magnetar Candidate XTE J1810-197. *ApJ* 629: 985–997. doi:10.1086/431476. arXiv:astro-ph/0505039.
- Yakovlev DG, Kaminker AD, Gnedin OY and Haensel P (2001), Nov. Neutrino emission from neutron stars. *Phys. Rep.* 354 (1-2): 1–155. doi:10.1016/S0370-1573(00)00131-9. astro-ph/0012122.
- Younes G, Kouveliotou C and Kaspi VM (2015), Aug. XMM-Newton Observations of SGR 1806-20 Over Seven Years Following the 2004 Giant Flare. *ApJ* 809 (2), 165. doi:10.1088/0004-637X/809/2/165. 1507.05985.
- Younes G, Kouveliotou C, Jaodand A, Baring MG, van der Horst AJ, Harding AK, Hessels JWT, Gehrels N, Gill R, Huppenkothen D, Granot J, Göğüş E and Lin L (2017), Oct. X-Ray and Radio Observations of the Magnetar SGR J1935+2154 during Its 2014, 2015, and 2016 Outbursts. *ApJ* 847, 85. doi:10.3847/1538-4357/aa899a. 1702.04370.
- Younes G, Baring MG, Kouveliotou C, Arzoumanian Z, Enoto T, Doty J, Gendreau KC, Göğüş E, Guillot S, Güver T, Harding AK, Ho WCG, van der Horst AJ, Hu CP, Jaisawal GK, Kaneko Y, LaMarr BJ, Lin L, Majid W, Okajima T, Pope J, Ray PS, Roberts OJ, Saylor M, Steiner JF and Wadiasingh Z (2021), Apr. Broadband X-ray burst spectroscopy of the fast-radio-burst-emitting Galactic magnetar. *Nature Astronomy* 5: 408–413. doi:10.1038/s41550-020-01292-x. 2006.11358.
- Zane S, Rea N, Turolla R and Nobili L (2009), Sep. X-ray spectra from magnetar candidates - III. Fitting SGR/AXP soft X-ray emission with non-relativistic Monte Carlo models. *MNRAS* 398: 1403–1413. doi:10.1111/j.1365-2966.2009.15190.x. 0906.1135.
- Zheleznyakov VV (1996). *Radiation in Astrophysical Plasmas*, 204, Kluwer Academic Publishers. doi:10.1007/978-94-009-0201-5.